COMOTI
ROMANIAN RESEARCH & DEVELOPMENT INSTITUTE FOR GAS TURBINES

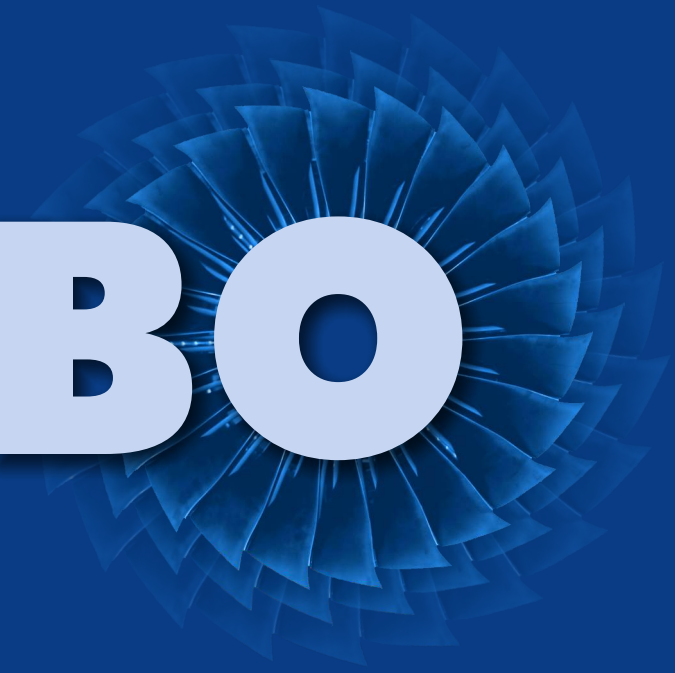

TURBO

Scientific Journal

vol. V (2018), no. 1

ROMANIA
1918 - 2018 | WE CELEBRATE TOGETHER!

In 1918, the Romanian National State was formed by unifying the Romanian Provinces with Romanian Kingdom. It all happened in multiple stages, first on 27th of March 1918 when Basarabia was unified with Romanian Kingdom, afterwards on 28th of November 1918 was joined by Bucovina and on the 1st of December 1918 were followed by Transilvania, Banat, Crisana and Maramures. This moment was considered the Great Union from 1918.

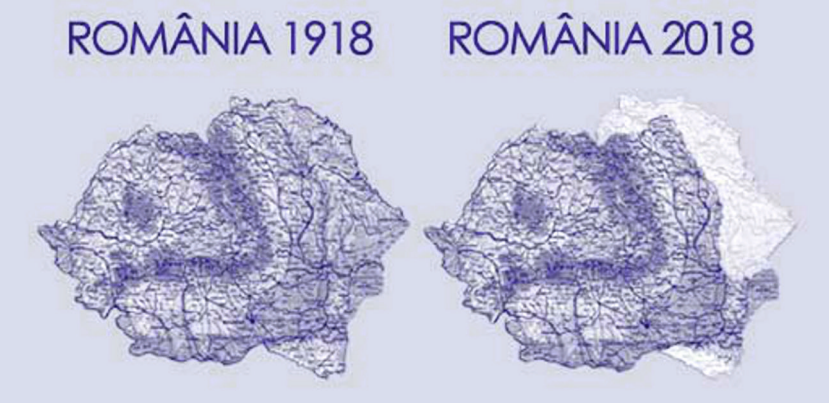

This day is celebrated until the present as The Grate Union's Date, particularly this year when 100 years have passed.

2018 is The Great Union's Centenary!

1918 is not important only for Romanian people, it is also an important year for World's Science:

- Heber Curtis discovers a relativistic jet of matter emerging from Elliptical galaxy M87;
- Arthur Scherbius applies to patent the Enigma machine;
- Edward Hugh Hebern patents the Hebern rotor machine;
- Technisches Museum Wien opens in Vienna;
- Gaston Julia describes the iteration of a rational function;
- Josef Lense and Hans Thirring find the gravitomagnetic precession of gyroscopes in the equations of general relativity;
- Hans Reissner and Gunnar Nordström solve the Einstein and Maxwell field equations for charged spherically-symmetric non-rotating systems;
- J. B. Christopherson publishes his discovery that antimony potassium tartrate is an effective cure for schistosomiasis;
- Edwin Armstrong invents the superheterodyne receiver;
- Theodore von Karman and Asbóth Oszkár build the first co-axial helicopter;
- A. M. Nicolson invents the radio crystal oscillator;
- Gogu Constantinescu published a book which was considered the birth of the Theory of Sonics.

EDITORIAL

Știința conduce progresul omenirii (1)

Armonia vieții sociale este rezultatul respectării principiilor societății și a normelor de interacțiune cu lumea înconjurătoare. Natura acestei armonii este strâns legată de una dintre cele mai presante probleme ale civilizației moderne: piața nevoilor sociale. Problema granițelor de consum există de mii de ani cu tendința de a deveni mai complexă pe măsură ce limitele se extind. Aici intervine rolul științei, prin creșterea cunoștințelor disponibile omului, care își sporește controlul asupra mediului înconjurător, permițându-i să-și folosească imaginația pentru a-și îmbunătăți starea și viața de zi cu zi.

Cel mai adesea cererea pentru știință și tehnologie este latentă și se exprimă într-un moment de necesitate. Când se îmbină conșientizarea omului de știință pentru interesul acordat de societate muncii sale cu această necesitate lucrurile pot deveni fericite, adăugându-se pași în evoluția societății.

Herbert Mc Luhan a prevăzut nașterea internetului cu 35 de ani înainte de apariție. El a descris istoria umană ca pe o succesiune de acte de extindere tehnologică a omului, fiecare dintre acestea realizând o schimbare radicală a mediului ambiental și a modurilor de a gândi, simți și evolua. În prezent necesitățile sociale se subordonează acestui nou tip de comunicare, care se bazează pe ieșirea liberă a individului în actualul câmp informațional. Accesibilitatea și libertatea utilizării informațiilor transformă spațiul media într-un loc de întâlnire pentru oamenii care își caută armonia în vasta lume a culturii moderne. Cum tendința de dizolvare în realitatea virtuală este în creștere, schimbările vor deveni din ce în ce mai evidente, fiecare aspect tehnic sau economic fiind de fapt rezultatul interacțiunii și contracarării nevoilor. Știința are relații strânse cu aspectele sociale, politice și economice ale funcționării societăților noastre, și nu putem lua în considerare activitatea științifică în afara lumii sociale care o face posibilă.

Filozofii antici, cunoscând natura umană au identificat determinarea socială prin împărțirea nevoilor în materiale și spirituale. Heraclit din Efes (535-475 î.Hr.) a studiat scopul social al aurului, datorită căruia era posibil schimbul, adică compararea nevoilor oamenilor cu nevoile societății, căci transformările materiale, credea el, au la bază aceleași nevoi umane însă în permanentă schimbare căci "nici un om nu poate să intre în apa aceluiași râu de două ori, deoarece nici râul și nici omul nu mai sunt la fel".

Încrederea în știință ca factor de progres, a fost dovedită în timp. Secolul XVII al Iluminismului a considerat știința binefăcătoare.

EDITORIAL

Știința conduce progresul omenirii (2)

Încrederea de care s-a bucurat atunci era absolută, cunoașterea fiind capabilă să răspundă la toate întrebările cu care se confrunta omul. În timp însă evoluțiile științei și tehnologiei nu au avut loc întotdeauna fără ciocniri sau dispute.

Iluminatul urban, vaccinarea în masă, au cunoscut o puternică opoziție, fapt care dovedește că implementarea unei tehnologii nu este niciodată câștigată în avans. În situațiile de război rezultatele prevalează și justifică adesea mijloacele folosite pentru a le atinge, așa cum a fost cazul cercetării în domeniul fizicii nucleare puternic susținută de Statele Unite.

Cu timpul rezultatele științifice au fost considerate bunuri ale societății mai ales în domeniile energiei, medicinei, transportului ori comunicațiilor. În secolul XIX termodinamica, asociată mecanicii și electricității, a condus la dezvoltarea locomotivelor și a sistemelor feroviare ceea ce a condus la creștere economică; economia are nevoie de știință așa cum justificarea filozofică a științei oferă accesul la rațional.

Istoricul și filozoful britanic Arnold J. Toynbee susținea că nu există embrioni culturali primordiali, ascensiunea culturală existând în soarta tuturor popoarelor, însă forma pe care o capătă este diferită. El a fundamentat sistemul "provocare-răspuns", în care schimbările publice sunt determinate de răspunsul societății la provocările care o fac să se schimbe. Provocarea în sine poate fi condiționată de factori naturali și sociali, la care minoritatea creativă, fără de care progresul nu poate fi conceput, este foarte receptivă.

Oamenii de știință, ale căror motoare intelectuale rămân înțelegerea și explicarea fenomenelor precum și îmbunătățirea vieții noastre de zi cu zi, se confruntă cu responsabilități care apar prin cunoaștere. Societatea contemporană, societate de risc, implică o reinventare a practicii, astfel încât rezultatele cercetărilor lor să poată contribui efectiv la progresul umanității.

Autor: Elena Banea

Iunie 2018

EDITORIAL

Science Leads to Human Progress (1)

A balanced social life derives from the observance of social principles and rules of interaction with the surrounding world. The nature of this balance is closely connected to one of the most stringent issue of modern civilization: the social needs market. The issue of consumption borders has been in line for ages, and it tends to become ever more complex while the limits expand continuously.

Here comes the role of science, which facilitates knowledge increase available to man, who constantly puts a stronger grip on the environment, thus being able to use his imagination in order to improve his condition and everyday life.

Most often than not, the demand for science and technology is being latent and it only becomes vocal in times of necessity. When there is a conjunction between the scientists' awareness of the interest of society in his work and this technological demand, things can take a good turn, while new steps are being made towards the evolution of society.

Herbert Mc Luhan foresaw the birth of the internet 35 years ahead its appearance. He described human history as man's successive steps towards technological development, each of them determining a radical change of his environment as well as of his way of thinking, feeling and progressing. Nowadays, social needs are subordinated to this new type of communication that is based on man's willing presence in the existent informational space. Accessibility and freedom of using information turns the media space into a convergence place for people who are looking for their balance in the wide world of modern culture. Since there is an increasing tendency for people to mergence into virtual reality, changes are due to become ever more evident, each technical or economic aspect being actually the result of interaction and counter reaction to human needs.

Science is strongly connected to the social, political and economic aspects of our society, and one cannot consider scientific activity outside the social world that makes it happen. Ancient philosophers, who were familiar with human nature, identified social determination by dividing the needs into material and spiritual ones.

Heraclit of Efes (535-475 B.C.) studied the social function of gold, which facilitated exchange, that is the comparison of individual needs with social needs, since material changes, he believed, basically came from the same human needs, though permanently changing, of course, as "no man can plunge twice into the same river water, since neither the river, nor the man will not be the same anymore."

EDITORIAL

Science Leads to Human Progress (2)

Reliance on science, as a factor of progress, has been proven in time. The 17th century or the Enlightenment considered science as a positive factor. Reliance on it was complete at that time, knowledge being able to answer all the problems that man confronted with back then. As time passed, though, science and technological evolution occurred not without conflicts or disputes.

Urban lightening and mass vaccination faced a strong opposition, which proves that the implementation of new technology is never won in advance. In conflicting situations, results prevail over and often justify the means used to achieve them, as in the case of research in nuclear physics strongly supported by the United States.

In time, scientific results turned out to be considered social goods, especially in such fields as energy, medicine, transportation or communication. In the 19th century, thermodynamics associated to mechanics and electricity led to the development of engines and railway systems, which contributed to economic growth; economy needs science, the same way as philosophical justification of science facilitates access to reason.

A British historian and philosopher, Arnold J. Toynbee, asserted that there were no primordial cultural embryos, cultural evolution being latent in the culture of all peoples, but that the form it takes is always different. He substantiated the "challenge-response" system, according to which public changes are determined by the public answer to the challenges that determine its change. The challenge, in itself, can be conditioned by natural and social factors, to which the creative minority, without which there is no progress, is extremely receptive to.

Scientists, whose intellectual gears will be the understanding and explanation of phenomena, as well as the improvement of our everyday lives, confront with various responsibilities that arise from knowledge. Contemporary society, a society that confronts with various risks, asks for the reinvention of practice, so that the results of their research may actually contribute to the progress of mankind.

Author: Elena Banea

June 2018

More information regarding the scientific journal can be found at:
http://www.comoti.ro/ro/jurnalul_stiintific_turbo.html
turbojournal@comoti.ro
jeni.popescu@comoti.ro

ISSN: 2559-608X
ISSN-L: 1454-2897

Scientific Journal TURBO is included in ICI World of Journals:
https://journals.indexcopernicus.com/search/details?id=48512

TABLE CONTENT

June 2018

PRELIMINARY CAMELINA OIL COMBUSTION TESTS ON A MICRO GAS TURBINE FIRE TUBE

Andreea MANGRA[1], Cornel SANDU[1], Marius ENACHE[1], Florin FLOREAN[1], Razvan CARLANESCU[1], Radu KUNCSER[1]

ABSTRACT: Camelina is well-suited to be a biofuel crop, as its seeds naturally have high oil content. At present, the process of obtaining bio-kerosene from camelina oil by hydrotreatment is time consuming and expensive, thus the possibility of using straight camelina oil as fuel in terrestrial applications is taken into consideration. For this purpose, combustion tests have been conducted on a micro gas turbine's combustion chamber. As fuels have been used a 50% camelina oil / 50% kerosene mixture and 100% camelina oil, both pre-heated at 90°C. The combustion chamber functioned satisfactorily on both fuels. In the future the tests will be resumed for other functioning regimes, varying the air mass flow, the air pressure and fuel mass flow. Also, the design of an injector dedicated to function on camelina oil is taken into consideration.

KEYWORDS: camelina oil, combustion tests, micro gas turbine, fire tube, exhaust gas analysis

NOMENCLATURE

P1 – pressure on the fuel delivery pipe (before the thermostatic oil bath)
P2 – pressure on the fuel bypass pipe
P3 – fuel pressure before the injector (after the thermostatic oil bath)

1. INTRODUCTION

In recent years, the global energy market has been influenced by the concern regarding global warming caused by greenhouse emissions and the reduction of fossil fuels supply. For these reasons, there is an increased interest in finding and using renewable and eco-friendly sources of energy

Camelina is an oilseed plant that grows optimally in temperate climates, thus it can be cultivated in Romania. Also, camelina is a promising energy crop due to its seeds high oil content [1]. Second generation bio-fuel has been obtained from camelina oil by hydrotreatment or Fischer-Tropsch synthesis [2]. The bio-kerosene obtained from camelina oil meets all the requirements regarding performance and safety [3] in order to be used in aviation applications. Starting from 2009, the American Air Forces have successfully tested blends of classic aviation fuel / bio-kerosene obtained from camelina oil on fighting planes [4]. Passenger air companies such as KLM and Japan Airlines have successfully conducted flights using as fuel mixtures of classic jet fuel and bio-kerosene obtained from camelina oil [4].

At the moment, the production of second generation bio-fuels is costly, requiring sophisticated equipment. According to the European Commission Directive 2009/28/EC, straight vegetable oils obtained by pressing from oil plants seeds, not chemically processed, are considered biofuels. Production costs of crude vegetable oils are much lower than those of transforming them into bio-diesel or bio-kerosene, thus leading to lower trading prices.

Up to present day researchers have investigated the possibility of using various vegetable

[1] National Research and Development Institute for Gas Turbines COMOTI, Bucharest, Romania

oils or biofuels obtained from these oils, as fuels for internal combustion engines [5, 6, 7, 8], for micro gas turbines [9, 10, 11, 12] or for furnaces and boilers [13, 14].

Regarding camelina oil, there have been reported results of using it as fuel in internal combustion engines [15, 16]. Burning behaviour and exhaust emission data revealed that straight camelina oil can be used as fuel on diesel engines, but not for long periods of time due to its high Conradson Carbon Residue (CCR) values and low oxidation resistance. Thus, the oil has to be supplemented with antioxidant additives.

Tests regarding the combustion of camelina oil /kerosene mixtures in a micro gas turbine have been reported in [17]. The following mixtures have been used as fuel: 10% camelina oil / 90% kerosene and 15% camelina oil / 85% kerosene. The mixtures have not been pre-heated. The conclusion was that in case of emergency the micro gas turbine can function using these mixtures as fuel. For longer operating periods the mixtures have to be pre-heated in order to lower their viscosity, getting it closer to the kerosene's viscosity.

The combustion tests presented in this article are a continuation of the research work presented in [18]. Straight camelina oil and camelina oil / kerosene mixtures have been tested on a burner. Based on an exhaust gas analysis it was concluded that fuel pre-heating temperature of 90°C is enough for an efficient combustion process. An increase of the fuel pre-heating temperature over this value does not improve significantly the combustion process.

Given all of the above, it was considered that the next step is to conduct combustion tests of pre-heated camelina oil on a micro gas turbine's combustion chamber. The purpose is to find out if pre-heated camelina oil can be used as fuel on such an engine, for terrestrial applications.

2. THE TESTING RIG

The testing rig on which the combustion experiments have been conducted is composed of: the fuel supply system, the fuel pre-heating system, the air source, the air electrical pre-heater, the combustion chamber assembly. The air necessary for the combustion tests has been delivered by an air-blower existent within the combustion laboratory.

Under real operating conditions of a micro gas turbine, the air delivered by its compressor reaches the combustion chamber at a higher temperature than the ambient temperature. Thus, during the combustion experiments, in order to be as close as possible to real functioning conditions, the air has been pre-heated using an electrical pre-heater. The air mass flow has been measured using a flow-meter positioned ahead of the electrical pre-heater. The maximum available air mass-flow in this section was of 0.13 kg/s.

The fire tube on which the tests have been conducted comes from a Garrett micro gas turbine model GTP 30-67 (Fig. 1 and 2). There have also been used the micro gas turbine's fuel injector and spark plug.

Fig. 1 The fire tube

Fig. 2 The fire tube interior

The fuel supply system (Fig. 3) consists of: a tank where the fuel is at room temperature, a pre-feed fuel pump, a fuel filter, a main fuel pump and valves both on the delivery pipe and on the bypass pipe. The fuel pressure, both on the delivery pipe and on the bypass pipe, is monitored using pressure gauges.

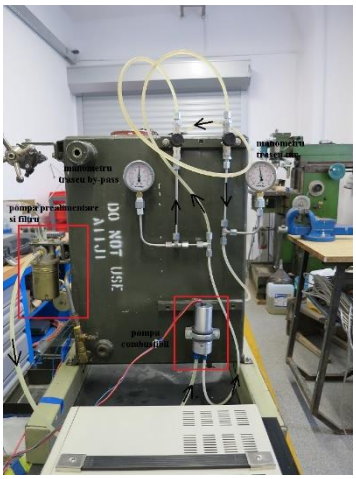

Fig. 3 The fuel supply system

The fuel pre-heating system (Fig. 4 and 5) consists of a thermostatic oil bath in which a coil, through which the cold fuel passes, is immersed. The oil in the bath is heated using an electrical resistance. Thus, the fuel in the coil is heated through heat transfer. The walls and lid of the oil bath are thermally insulated with fibre glass in order to minimize the heat loss.

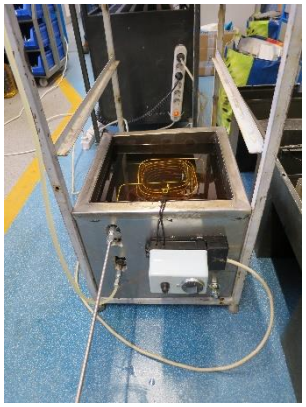

Fig. 4 The fuel pre-heating system

Fig. 5 The oil bath interior

The fuel temperature and pressure are monitored using a thermocouple, respectively a manometer, placed on the fuel line after the thermostatic oil bath (Fig. 6).

For safety measures a stop valve has been placed on the fuel line before the injector in order to be able to cut the fuel supplying (Fig. 6).

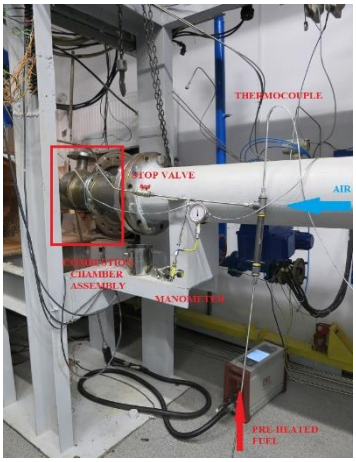

Fig. 6 The fuel supply line instrumentation

At the fire tube exit both the exhaust gas temperature and its composition are monitored using a gas analyzer.

A schematic representation of the whole testing line is presented in Fig. 7.

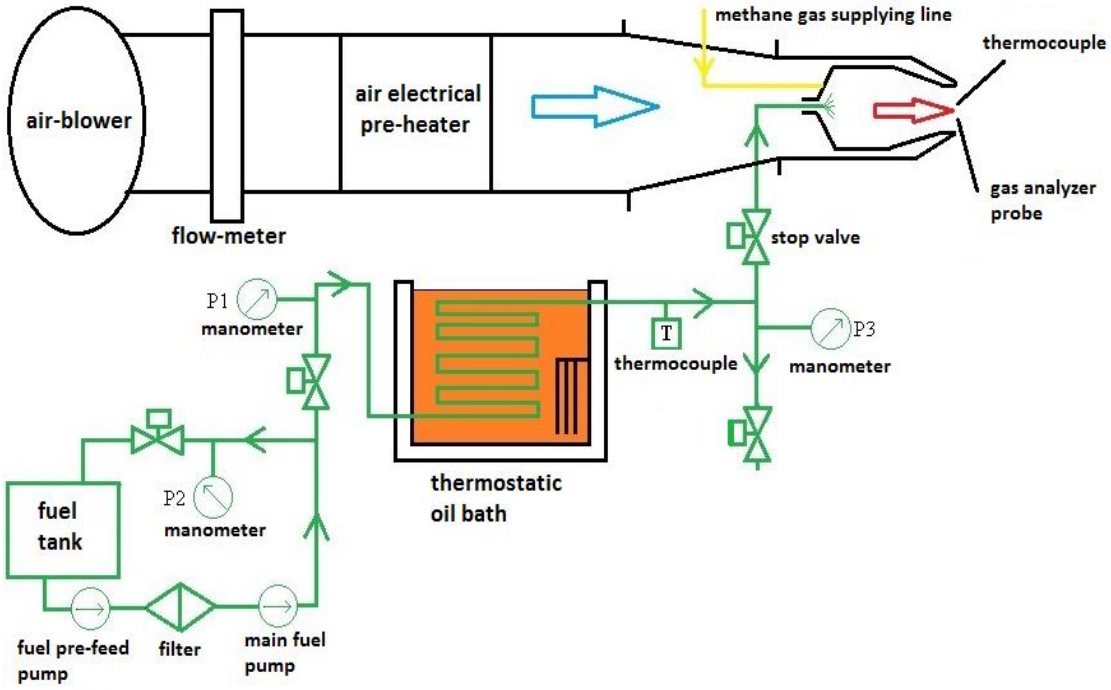

Fig. 7 Schematic representation of the testing line

3. TESTED FUNCTIONING REGIMES

The combustion tests have been conducted at atmospheric pressure. The air delivered by the air-blower has been pre-heated at 130°C, calculated based on the engine data [19].

The combustion chamber was first fuelled with kerosene. The fuel's injection pressure p3 has been increased in order to obtain a suitable spraying of the fuel. In the same time the temperature at the combustion chamber exit was monitored so that it would not exceed 1100°C. The air mass flow has been gradually increased to its maximum of 0.13 kg/s.

In these conditions it was possible to increase the pressure up to 3 bars. Thus, it was obtained a spraying cone of approximately 40° (Fig. 8 a)). According to the micro gas turbine's technical manual [19], for this injector a suitable spraying cone has to be of at least 70°. Based on these observations, in the future the tests will be resumed using an air source capable to deliver a higher mass flow.

Next the combustion chamber was fuelled using a 50% camelina oil / 50% kerosene mixture (Fig. 9 a)). The fuel mixture has been pre-heated at around 90°C in order to lower its viscosity. This pre-heating temperature was chosen based on combustion tests results presented in [20]. The same procedure as in the case of 100% kerosene was followed.

The fuel's injection pressure was gradually increased, in the same time monitoring the fire tube exit temperature so that it would not exceed 1100°C. The air mass flow was set at 0.13 kg/s. In these conditions it was possible to increase the pressure up to 5 bars. Thus, it was obtained a spraying cone of approximately 60° (Fig. 8 b)).

Next the combustion chamber was fuelled using 100% camelina oil (Fig. 9 b)). The oil has been pre-heated at around 90°C in order to lower its viscosity. This pre-heating temperature was chosen based on combustion tests results presented in [20].

In these conditions it was not possible to ignite the fuel using only the spark plug. The solution was to fuel the combustion chamber in parallel with methane gas and pre-heated camelina oil. After the flame was stabilized the methane gas supplying was stopped gradually, letting the combustion chamber to function only on camelina oil.

The fuel's injection pressure was gradually increased, in the same time monitoring the fire tube exit temperature so that it would not exceed 1100°C. The air mass flow was set at 0.13 kg/s. In these conditions it was possible to increase the pressure up to 6.6 bars. Thus, it was obtained a spraying cone of approximately 50° (Fig 8 c)).

a) b) c)

Fig. 8 Spraying cone: a) kerosene, b) 50% camelina oil / 50% kerosene pre-heated at 90°C, c) camelina oil pre-heated at 90°C

a) b)

Fig. 9 The fire tube exit: a) 50% camelina oil / 50% kerosene, b) camelina oil

Based on these results it was observed that in order to obtain the same spraying cone angle, in the case of pure camelina oil it was necessary a greater fuel injection pressure than in the case of the camelina oil / kerosene mixture. This can be explained by the higher camelina oil's viscosity in comparison with that of the camelina oil / kerosene mixture [21].

Also, in the case of the camelina oil /kerosene mixture even though the injection pressure is lower than in the case of pure camelina oil, it can be observed a more suitable atomization of the fuel. This can be explained by the fact that the used injector was designed to function properly on kerosene. The camelina oil has different thermo-physical properties than kerosene, thus it was expected that the atomization process to be negatively influenced. The camelina oil /kerosene mixture thermo-physical properties are closer to those of kerosene, this leading to a better atomization process in this case.

In Table 1 a list of the tests performed on the test rig is presented.

Table 1. Tested functioning regimes

Fuel	P1[bar]	P2[bar]	P3[bar]	Air temp. [°C]	Fuel temp. [°C]	Air mass flow [kg/s]	Fuel mass flow [kg/s]
100% kerosene	3	3.4	3	130	15	0.13	0.00236
50% camelina oil / 50% kerosene	5	5.4	5	130	90	0.13	0.00286
100% camelina oil	8	9	6.6	130	90	0.13	0.00514

During the combustion tests significant tar deposits have been observed on the fire tube's interior walls (Fig. 10). This is a sign of a poor combustion process, for the given functioning regimes. These tar deposits are unburned hydrocarbons result of an incomplete combustion process. This is caused by the camelina oil's and

camelina oil / kerosene mixture's higher viscosity than that of pure kerosene. This leads to a poor atomization of the fuel resulting high diameter droplets which cannot be vaporised. This can be improved by increasing the fuel injection pressure. This will be taken into consideration for future combustion tests.

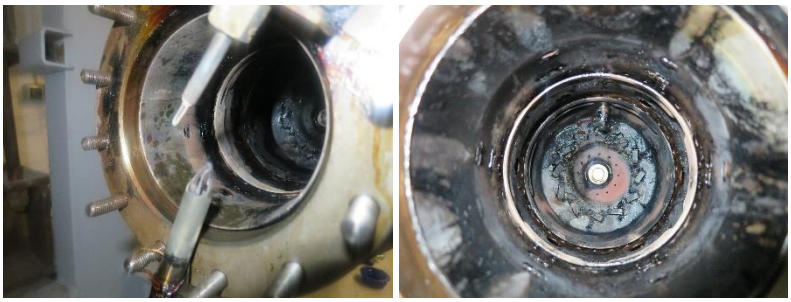

Fig. 10 Tar deposits on the fire tube's interior walls

4. EXHAUST GAS COMPOSITION ANALYSIS

During the combustion tests, the exhaust gas temperature and the concentrations of CO, CO_2, NO_x and O_2 in it have been monitored using a MRU Vario Plus gas analyser. The gas analyser can record with a frequency of 1 reading/second [22].

In figures 11-15 are presented the exhaust gas temperature and the CO, CO_2, NO_x and O_2 concentrations in it for the tested functioning regimes.

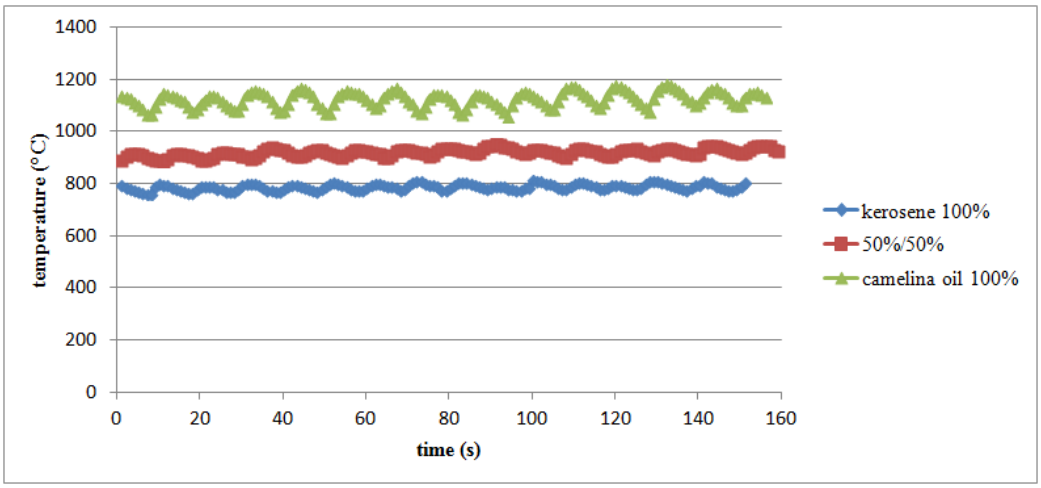

Fig. 11 Exhaust gas temperature

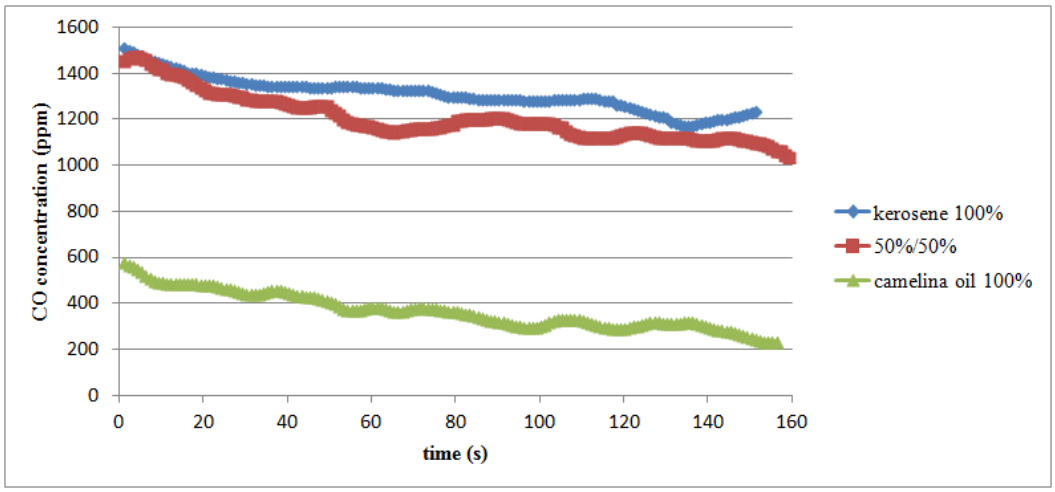

Fig. 12 CO concentration

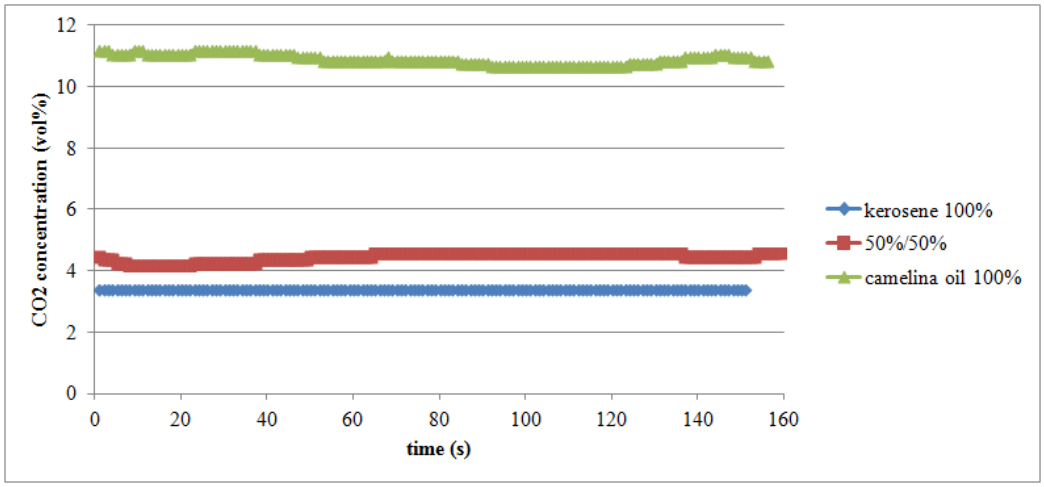

Fig. 13 CO_2 concentration

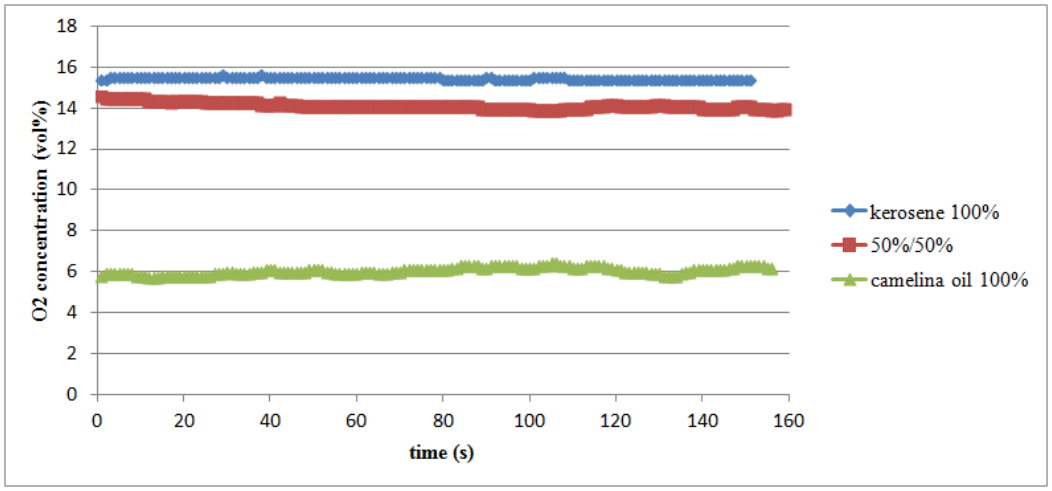

Fig. 14 O_2 concentration

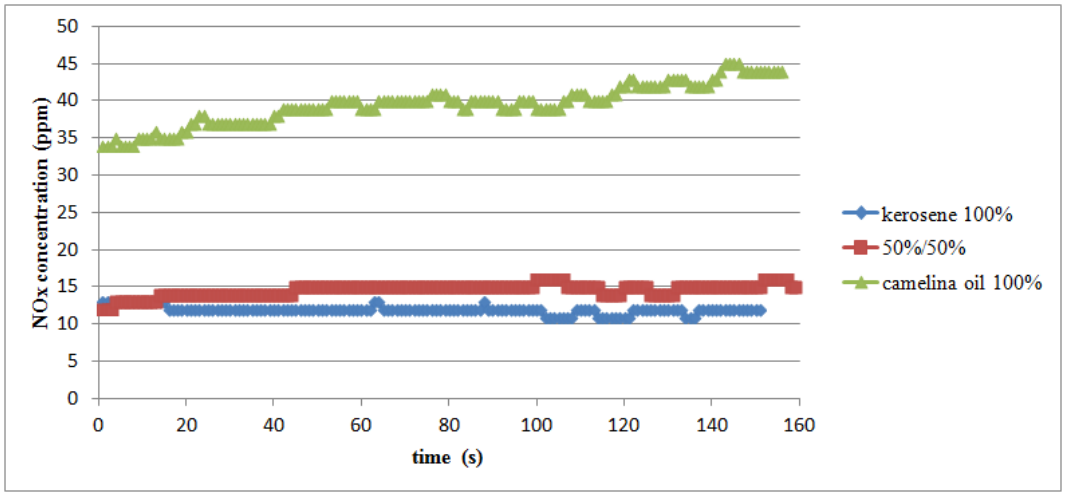

Fig. 15 NOx concentration

The exhaust gas temperature oscillations observed in Fig. 11 could be explained by the fact that the pre-heated air temperature is not constant, varying with ±5 around 130°C. In the cases of the camelina oil / kerosene mixture and straight camelina oil the temperature oscillations are greater. This is caused by additional variations of the pre-heated fuel's temperature. By pre-heating the fuel its viscosity is lowered, thus influencing its atomization. A better spraying of the fuel leads to an increase of the exhaust gas temperature. There is also observed a good correlation between the exhaust gas temperature and the CO and NO_x concentrations. An increase of the exhaust gas temperature leads to a decrease of the CO concentration and an increase of the NO_x

concentration. In a combustion process, the most important amount of heat is released during the oxidation of carbon monoxide into carbon dioxide [23]. Therefore, exhaust gases with a high CO concentration will have lower temperatures. On the other hand, the growth of the exhaust gases temperature favours the dissociation of the nitrogen molecules which leads to the formation of the nitrogen oxides [23].

The trend followed by the CO_2 concentration is also in good correlation with the behaviour of the exhaust gases temperature. The concentration increases with the increase of the temperature, this being an effect of the combustion process improvement.

From Fig. 14 it can be seen that the O_2 concentration behaviour is in accordance with the trend followed by the CO concentration, the O_2 concentration decreasing with the decrease of the CO concentration. This is caused by the larger quantities of O_2 and CO consumed to create the CO_2.

5. CONCLUSIONS

The results of these preliminary combustion test are encouraging. There have been some problems in the ignition phase when straight camelina oil has been used. But after that, the combustion process has been stable and the flame did not extinguish. For the given functioning regimes, the CO concentration was much lower when camelina oil has been used as fuel. On the other hand, NO_x concentration was higher due to the higher temperature of the exhaust gas.

The air necessary for these preliminary combustion tests has been delivered at atmospheric pressure. For future research it is desired to resume the combustion tests at higher air pressures. For this particular fire tube, it is desired to reach at an air pressure of 3 bars so that to be in accordance with the micro gas turbine's technical characteristics [19].

Also, the tests will be resumed using an air source capable to deliver higher mass flows. A higher air mass flow leads to the possibility of using a higher fuel mass flow without the combustion chamber exit temperature exceeding values of 1100°C. A higher fuel mass flow leads to the increase of the injection pressure thus improving the fuel spraying. The tests, for the given functioning conditions, showed that the fuel spraying was not adequate. There have been obtained spraying cones of 50°. From the injector's technical data [19], a suitable spraying cone must be of at least 70° and this can be obtained only by increasing the injection pressure.

ACKNOWLEDGEMENT

This work was carried out within “Nucleu” Program TURBO 2020, supported by the Romanian Minister of Research and Innovation, project number PN 16.26.01.09

REFERENCES

[1] Moser B.R., 2012, Biodiesel from alternative oilseed feedstocks: camelina and fiels pennycress, *Biofuels* vol. 3, pp. 193-209
[2] A. Bauen, J. Howes, L. Bertuccioli, C. Chudziak, 2009, *Review of the potential for biofuels in aviation*, final report for The Committee on Climate Change, E4tech
[3] J.D.Kinder, T. Rahmes, 2009, *Evaluation of bio-derived synthetic paraffinic kerosene*, The Boeing Company, Sustainable Biofuels Research & Technology Program
[4] Eynck C., Falk K.C., 2013, Camelina, Editor: Singh B.P., *Biofuel Crops. Production, Physiology and Genetics*, CABI, pp. 369-392
[5] Hartmann R., Garzon N., Hartmann E., et al, 2012, Vegetable oils of soybean, sunflower and tung as alternative fuels for compression ignition engines, International Conference on Efficiency Cost Optimization Simulation and Environmental Impact of Energy Systems (ECOS 2012), Perugia, Italy, 26-29.06.2012
[6] Hazar H., Aydin H., 2010, Performance and emission evaluation of a CI engine fuelled with preheated raw rapeseed oil (RRO)-diesel blends, *Applied. Energy*, vol. 87, no. 3, pp. 786-790
[7] Chalatlon V., Roy M.M., Dutta A., Kumar S., 2011, Jatropha oil production and an experimental investigation of its use as an alternative fuel in a DI diesel engine, *Journal of Petroleum Technology and Alternative Fuels*, vol. 2, no. 5, pp. 76-85
[8] Drenth A.C., Olsen D.B., Cabot P.E, Johnson J.J., 2014, Compression ignition engine performance and emission evaluation of industrial oilseed biofuel feedstocks camelina, carinata, and pennycress across three fuel pathways, *Fuel*, vol. 136, pp. 143-155

[9] Cavarzere A., Morini M., Pinelli M., Spina P.R., Vaccari A., Venturini M., 2012, Fuelling micro gas turbines with vegetable oils. Part II: Experimental analysis, ASME Turbo Expo 2012, Copenhagen, Denmark, 11-15.06.2012
[10] Chiaramonti D., Rizzo A.M., Spadi A., Prussi M., Riccio G., Martelli F., 2013, Exhaust emissions from liquid fuel micro gas turbine fed with diesel oil, biodiesel and vegetable oil, *Applied Energy*, vol. 101, pp. 349-356
[11] Y. Schmellekamp, K. Dielmann, 2004, Rapeseed oil in a Capstone C30, *Workshop: Bio-fuelled Micro Gas Turbines in Europe*, Brusseles, Belgium, 24.09.2004
[12] Rosa do Nascimento M.A., Cruz dos Santos E., 2011, Biofuel and gas turbine engines , editor: Benini E., *Advances in Gas Turbine Technology*, Intech
[13] Oprea I., Mihaescu L., Prisecaru T., Negreanu G.P., Georgescu M.E., Popa E., 2008, Experimental reserach on crude vegetable oil combustion in a small boiler – 55 kW, *Termotehnica*, vol. 2, pp. 65-69
[14] Thuneke K., Widmann B., 2001, Operational reliability of vegetable oil fuelled central heating plants, *Landtechnik*, vol.56, no. 4, pp. 334-335
[15] Bernardo A,, Howard-Hildige R., O'Connell A., Nichol R., Ryan J., Rice B., Roche E., Leahy J.J., 2003 Camelina oil as a fuel for diesel transport engines, *Industrial Crops and Products*, vol. 17, pp. 191-197
[16] Paulsen H.M., Wichmann V., Shuemann U., Richter B., 2011, Use of straight vegetable oil mixtures of rape and camelina as on farm fuels in agriculture, *Biomass and Bioenergy*, vol. 35, pp. 4015-4024
[17] Petcu A.C, Sandu C., Berbente C., 2014, Combustion of Camelina oil – kerosene mixtures in a micro gas turbine, *Modeling and Optimization of the Aerospace, Robotics, Mechatronics, Machines-Tools, Mechanical Engineering and Human Motricity Fields*, vol. 555, pp. 102-107
[18] Petcu A.C., Florean F.G., Porumbel I., Berbente C., Silivestru V., 2016, Experiments regarding the combustion of camelina oil/kerosene mixtures on a burner, *Energy for Sustainable Development Journal*, vol. 33, pp. 149-154
[19] ***, „Shaft Power Gas Turbine Engine. Mode GTP 30-67," Technical Manual, 1966
[20] Petcu A.C., 2016, Cercetari privind utilizarea uleiului de camelina drept combustibil (Research regarding the use of camelina vegetable oil as fuel), doctoral thesis, Politehnica University of Bucharest, Bucharest
[21] Petcu A.C., Cârlănescu R., Berbente C., 2014, Straight and Blended Camelina Oil Properties, 5th International Conference on FLUID MECHANICS and HEAT & MASS TRANSFER, Lisbon, Portugal, 30.10-01.11.2014, pp. 160-167
[22] ***, *Operating Manual MGA5 & VarioPlus Industrial*, MRU Emission Monitoring Systems
[23] Lefebvre A.H., Ballal D.R., 2010, *Gas Turbine Combustion. Alternative Fuels and Emissions*, 3rd edition, CRC Press, New York

NUMERICAL SIMULATIONS OF PULSE COMBUSTION IN SCHUBERT PULSEJET ENGINES

Ovidiu TROFIN[2], Andreea MANGRA[2], Eusebiu HRIȚCU[2], Gabriel URSESCU[2]

ABSTRACT: Currently, there is no mathematical model or procedure for designing a pulsejet engine that provides sufficient accuracy to be used in practice. For this reason, the paper addresses the problem by achieving a CFD study of a pulsejet in various configurations, starting from a simpler model (the Schubert model), in order to ensure the simple validation of the results through experimental study. Following the analysis of the results it can be concluded that the proposed method can be an effective tool for the design of pulsejet engines.

KEYWORDS: propulsion, combustion chamber, pulse combustion, pulsejet, numerical simulation.

NOMENCLATURE
All variables are defined throughout the work.

1. INTRODUCTION

The pulsejet is one of the simplest engines currently in existence and does not require complex technology to achieve. This gives it a high potential of use.

Despite many theoretical approaches, there are no mathematical models and design procedures to give full satisfaction in practice. The existing literature presents a number of experimental studies, but they are also limited due to the harsh conditions of such an engine.

Developing an appropriate mathematical model of working processes in a pulsejet engine involves describing the physical phenomena that govern the occurrence of periodic combustion in such motors. Different authors associate the occurrence of pulsating combustion with phenomena of waving, acoustic or turbulent nature, each of these approaches making it possible to describe certain characteristics of the pulsating burning process that can not be determined by other methods but at the same time have a number of disadvantages inherent to the accepted physical model.

Consequently, the theoretical studies on this type of propulsion system need to be continued.

The pulsejet engine is influenced by the acoustic phenomena that occur during operation, making it very sensitive to the geometry of the combustion chamber, the exhaust and intake pipes. Although the engine is simple, the design of a pulsejet is complex and the achievement of an optimal geometric configuration presents difficulties.

Also, the experimental study of this kind of engines is hitting the difficulty of collecting the internal parameters (especially the temperature) due to its very high values, the limited space and the non-stationary operating mode of this type of engine.

The purpose of this paper is to develop a CFD model valid for simulating the operation of a pulsejet and which can be used at a later stage to estimate engine performance. This goal is in line with the general objective of developing a design principle for this type of engine and finding optimal configurations for different applications and in different environments.

[2] National Research and Development Institute for Gas Turbines COMOTI, Bucharest, Romania

2. PAPER CONTENTS

2.1. General considerations

The present paper aims at generating a viable CFD model for simulating the thermo gas dynamics phenomena that takes place during the operation of a pulsejet and using this model to predict and optimize the operation of such an engine.

The objective is to develop the principles of designing a pulsejet and to generate solutions to optimize its operation.

In view of the above, several simple configurations were studied in the simulations, starting from one of the simplest types of pulsejet, namely the one developed by William Schubert in the 1940s (Figure 1).

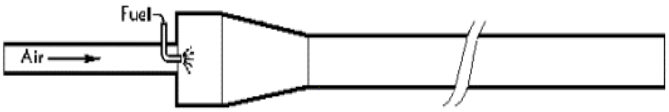

Fig. 1 Schubert pulsejet

As one can see, this type of pulsejet consists of three main parts: the intake tube, the main body (combustion chamber) and the exhaust pipe. Fuel intake is provided by an injector on the engine axis at the entrance of the combustion chamber to allow efficient mixing with the intake air.

Due to constructive simplicity, the configurations of the one in Figure 1 require relatively small resources for CFD modeling and simulation, which is the reason for selecting this type of pulsejet as a starting point.

2.2. Geometric configurations studied

The first configuration studied - C1 – is the one shown in Figure 2:

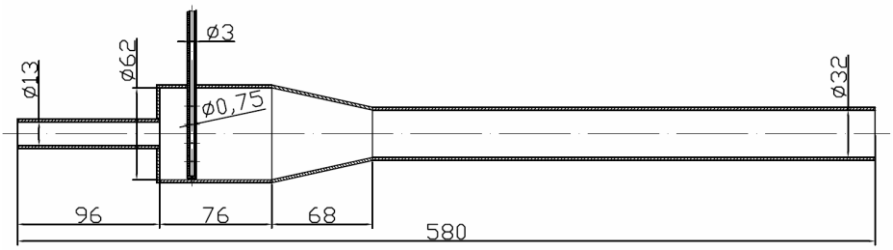

Fig. 2 Configuration C1

As one can see, the first configuration does not differ from the Schubert model except for the fuel injection mode. Thus, the injection is made by a tube perpendicular to the engine axis, provided with 8 holes of 0.75 mm diameter perpendicular to the general direction of air flow through the engine.

The second configuration - C2 - differs from the first one only through the diameter of the intake tube, which in this case has a value of 16 mm.

2.3. Boundary conditions

The computational domain is outlined in Figure 3. The computational domain covered not only the interior of the engine but was extended outward so that the simulation also captures the flow outside the engine. Knowing that the vertical plane passing through the axis is a symmetry plane, the considered computational domain represents only 180 degrees instead of the entire volume (360 degrees) for both geometric models studied.

In this paper, the ANSYS CFX ™ software package available in INCDT COMOTI was used to model the combustion process and flow phenomena inside and outside the pulsojet.

Because the geometric boundaries of the domain were chosen to be far from the model, the effects of the pulsejet operation on the external flow were considered negligible. The conditions imposed on the geometric limits of the range were temperature T_0 = 288 K and pressure p_0 = 105 Pa.

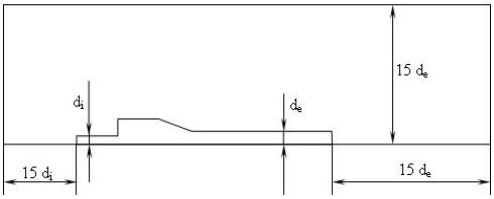

Fig.3 Computational domain

The temperature of the pulsejet wall was considered equal to the ambient temperature at the start of the simulation, in order to capture the operation of the engine from ignition to entering the mode. The temperature of the walls will increase over time due to heat exchange with the internal gases, and will stabilize once the engine enters the regime.

The simulation procedure was initiated by adopting 288K in the entire computing range at baseline. Also, null speed was imposed at any point in the field.

The simulation begins by introducing a propane flow of 0.05 g/s into the combustion chamber, which will be lit when the stoichiometric mixture is reached. This leads to a temperature and pressure jump that initiates the pulsating operation of the engine.

The simulation time step was 10^{-5} s, the data being stored at each iteration.

2.4. Performing and testing the mesh

Numerical simulations of acoustic resonators are addressed in numerous publications [1, 2, 3, 4, 5, 6, 7].

The mesh was generated in the entire computational domain. Inside the pulsejet it is much dense than the one generated for the outside of the pulsejet.

Figure 4 shows an image of the mesh network generated for the entire computational domain and for the combustion chamber area.

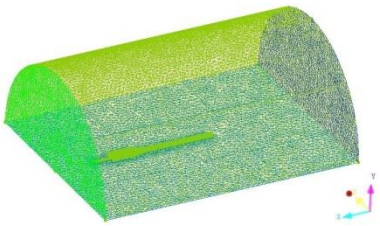

a. computational domain

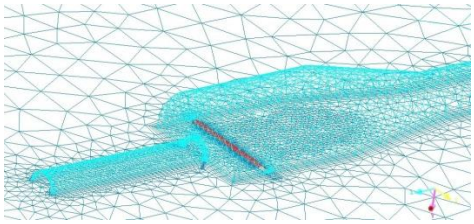

b. detail

Fig.4 The mesh network

2.5. Calculation assumptions used in simulations

Combustion and turbulence patterns were chosen from existing software models. However, the detailed knowledge of the working principle and the performance of the models used is necessary to understand the simulation results and the limits and errors of these calculation models.

The turbulence model "k - ε" was used to model the flow in the simulation of the pulsejet operation. For general purpose simulations, the "k - ε" turbulence model offers a good compromise on the accuracy of the results and the robustness of the calculation model. [8].

Combustion model

The fuel used is propane. A propane-air five step reaction mechanism (propane oxidation, hydrogen oxidation, CO oxidation, and both directions of water-gas shift reaction) provided by CFX was used to simulate the combustion process.

The chemical reaction rate is assumed to be relatively faster than the speed of transport processes in the flow phenomenon the Eddy dissipation model is thus used to simulate the combustion process. The model assumes that the reaction rate can be directly related to the time it takes to mix the reactants at the molecular level. When reactants mix at the molecular level, they instantly form products. In turbulent flows, this mixing is dominated by the swirling properties and therefore the reaction rate is proportional to a mixing time defined by the turbulent kinetic energy - k and the dissipation -ε.

Due to its simplicity and good performance in the modeling of turbulent reactive flows, the swirl pattern was widely applied in turbulent flame analysis. [9]

Acoustic model

Self-compression is one of the most important characteristics of pulsejets, so understanding this phenomenon is of considerable interest. Pressure oscillations in a pulsejet are amplified by an acoustic resonance.

Traditionally, a valved pulsejet is modeled as a tube closed at the valve end and opened at the exhaust end, so the fundamental resonance occurs when the total length of the pulsejet is equal to one-quarter of an acoustic wavelength.

In our case, the model studied was a valveless pulsejet and the inlet length was much shorter than the exhaust, only a few diameters long, and thus much shorter than the sound wavelength. The volume of the inlet is also small compared to the volume of the combustion chamber. Therefore, the combination of this short inlet and combustion chamber is modeled as a Helmholtz resonator. The frequency of a Helmholtz resonator is calculated as: [10]

$$f_i=[c_i/(2\pi)]\cdot[S_i/(VLi)]^{0.5} \quad (1)$$

where:

fi is the resonance frequency associated with the inlet,

ci is the average speed of sound in the inlet and combustion chamber,

Si is the cross section area of the inlet,

V is the volume of the combustion chamber,

Li is the length of the inlet.

Since the reactant mixture in the pulsejet has similar heat ratio and specific gas constant to that of air, in this paper, the speed of sound was calculated by assuming a γ (at the appropriate average temperature) and *R* for air.

The value of the operating frequency, calculated with relation (1), was used to check the frequency obtained by the numerical simulation.

2.6. Results

Configuration C1

The first simulation consisted of the C1 configuration (Figures 5a and 5b). It has been found that in this configuration, the entry conditions have been reached after about 13.7 ms. During this start-up period, the temperature in the combustion chamber fluctuates due to the uneven distribution of the mixture and the occurrence of ignition conditions at various points on the gas-dynamic path. After this moment a significant temperature drop occurs, followed by the discharge of a gas stream through the intake tube.

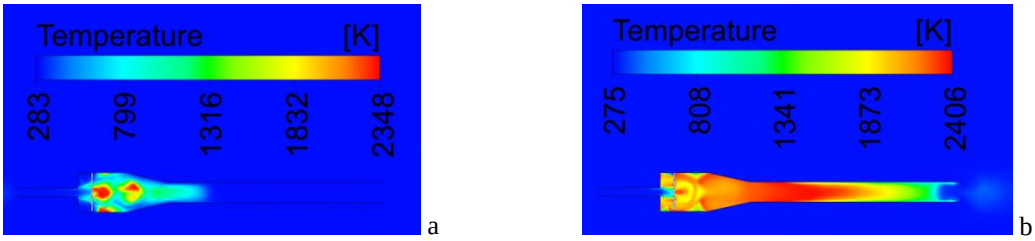

a b

Fig. 5. The temperature field in the C1 configuration

Next, the pressure drops inside and a fresh air stream is sucked in. The next explosion leads to exhaust gas evacuation both through the exhaust and intake, and the pulse operation is initiated (Figure 5b).

Figure 6 shows the variation of oxygen and combustion components concentrations during simulation of the C1 configuration.

It can be noticed that the temperature increase seen in Figure 5 is due to the initiation of the combustion process (around 13.7 ms), a phenomenon associated with a decrease in the percentage of oxygen in the fluid, simultaneously with the increase in the concentration of combustion products (H_2O and CO_2).

The second significant intensification of the combustion process takes place around the moment t = 28.5 ms, after which the process follows a cyclical evolution. It is possible to distinguish even from this graph the phases of the pulsating process: the aspiration is accompanied by the restoration of the oxygen concentration in the gases, after which the firing phase is initiated, the decrease of the oxygen level and the increase of the combustion products, followed by the increase of the pressure, evacuation and a new intake.

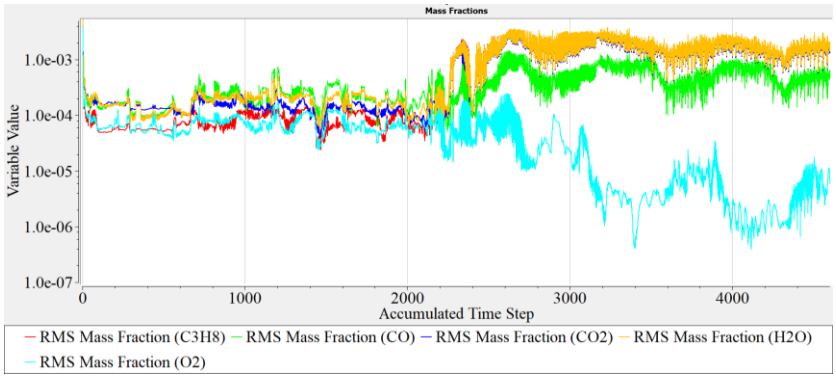

Fig. 6. The variation in time of the mass fractions of the chemical species in the C1 configuration

However, the oscillation period is not rigorously constant, a sign that the engine has not yet reached stable operating conditions. For stable operation, it is necessary for the walls of the combustion chamber to reach the operating temperature, which requires a longer operating time. However, it is noted that of the two complete oscillations captured in the figure, the first has a period of approx. 6.75 ms and the second of approx. 7.05 ms. This suggests an oscillating frequency of around 145 Hz.

The maximum temperature reached in the simulation was 2312,7K (figure 5), corresponding to the moment t = 28,6 ms, which also coresponds to a local minimum in terms of the oxygen concentration in the gas, ie the end of a combustion cycle.

Configuration C2

From the analysis of the variation of the combustion compounds (Figure 7), it results that in this configuration, the pulsating operation is initiated in 20.6 ms. It is also observed that the operating frequency is relatively more stable than in the first configuration, and is around 135 Hz.

The limited time available for the simulation did not allow the observation of the frequency stability. To determine the begining of the constant pulsed operation, simulation should be continued.

However, a change in working frequency over the previously studied configuration is observed, due to the increased diameter of the intake duct, which results in a change in the flow rate of the engine.

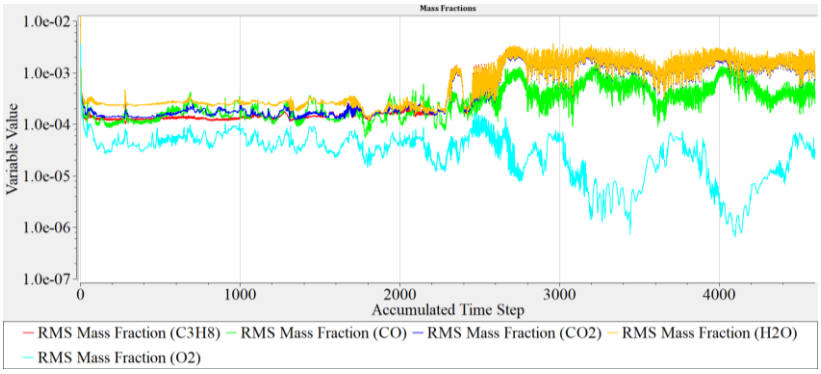

Fig. 7. The variation in time of the mass fractions of the chemical species in the C2 configuration

3. CONCLUSIONS

Following the elaboration of the paper, the following conclusions can be drawn:

- The purpose of the paper was to develop a CFD simulation procedure in the dynamic regime of thermogasdynamic processes that govern the operation of a pulsejet engine. From this point of view, the aim has been achieved, the resultant simulation process leading to phenomenologically predictable results. Of course, the elaborated process requires experimental validation, a process that will take place in the next stage.
- Even with the reduced complexity of the geometry associated with a pulsejet, the studied models required a long simulation time, due, not least, to the computing resources.
- Two geometric configurations have been studied, all starting from the Schubert pulsejet model. All models were simulated under the same outer and limit conditions, using the same fuel: C3H8. The burning model was the one in the Ansys CFX simulation program library. The differences between the configurations concerned in particular the engine intake area and the fuel system geometry.

- The two simulated configurations (C1 and C2) were simulated until the stable pulse operation was reached. The simulations showed the modification of the operating mode due to the geometry differences between the two configurations, even though they only concerned the diameters of the suction sections in the engine. The main difference in operation is the decrease of the working frequency with the increase of the suction section.
- All simulations were initiated, provided the walls of the combustion chamber were at ambient temperature, to simulate the pulse-starting conditions. In practice, the stable operation of a pulse reactor starts with the working temperature of the walls of the combustion chamber, which usually happens after a relatively long time (in the order of seconds). CFD simulation of the wall heating phenomenon consumes a very long time. Consequently, future simulations must begin at a much higher wall temperature, close to the actual operating mode.
- The simulations performed show the potential of the method. It captures the differences between the different geometric configurations and the results are in line with the practice from the perspective of the experience gained by the development team in the field of pulsejet engines. From a quantitative point of view, the method requires validation with practical experiments.

ACKNOWLEDGEMENTS

This work was carried out within "Nucleu" Program TURBO 2020, supported by the Romanian Minister of Research and Innovation, project number PN 16.26.08.05.

REFERENCES

[1] Wan, Q., Roberts, W. L., and Kuznetsov, A. V., *Computational Analysis of the Feasibility of a Micro-Pulsejet*, International Communication Heat Mass Transfer, 32, 2005, pp. 19–26.
[2] Geng, T., Kiker, A., Ordon, R., Schoen, M., Kuznetsov, A. V., Scharton, T., and Roberts, W. L., *Experimentation and Modeling of Pulsed Combustion Engines*, Four Joint Meeting of the US Sections of the Combustion Institute, 2005, Philadelphia.
[3] Geng, T., Schoen, M. A., Kuznetsov, A. V., Roberts, W. L., *Combined Numerical and Experimental Investigation of a 15-cm Valveless Pulsejet*, Flow & Turbulent Combustion, 78, 2007,
pp. 17–33.
[4] Kailasanath, K., Gardner, J., Oran, E., Boris, J., *Numerical Simulations of Unsteady Reactive Flows in a Combustion Chamber*, Combustion & Flame, 86, 1991, pp. 115–134.
[5] Chun, Y., and Kim, Y., *Numerical Analysis for Nonlinear Resonant Oscillations of Gas in Axisymmetric Closed Tubes*, J. Acoust. Soc. Am., 108, 2000, pp. 2765–2774.
[6] Sugannya Rose, *Design and Analysis of Improved Pulse Jet Engine*, International Journal of Scientific Engineering and Technology Research, Vol. 03, Issue 9, September 2014.
[7] Sai Kumar, Srinivas Prasad, Vamsi Krishna, *Design of Pulse Jet Engine for UAV*, International Journal of Scientific Engineering and Technology Research, Vol. 04, Issue 14, June 2015, pg. 2684–2687.
[8] ANSYS CFX - *Turbulence and Wall Function Theory*, ANSYS CFX Solver Theory Guide, 2013, pg. 84-85.
[9] ANSYS CFX - *Combustion Theory*, ANSYS CFX Solver Theory Guide, 2013, pg. 269-307.
[10] Rossing, T. D., and Fletcher, N. H., *Principles of Vibration and Sound*, Springer-Verlag, 2004, New York, pp. 216–219.

SIMULATING GEAR TOOTH CRACK PROPAGATION USING FEA

Andreea ALCEA[3], Răzvan BORCEA[3], Alexandru ILIEȘ[3], Ramona STANCIUC[3]

ABSTRACT: This paper present a simulation of a crack propagation using the maximum energy release rate criterion and j-integral parameter. The prediction is performed on a gear tooth under a variable load cycle in the elastic and elasto-plastic domains. A comparison based on the maximum tangential stress criterion is also presented. An analysis of the efficiency of the j-integral method in the elastic and elasto-plastic domains is also performed. The effect of the plastic deformation occurring close to the crack tip is considered while expressing the effective stress intensity factor as a function of the j-integral.

KEYWORDS:crack propagation, gear tooth, elasto-plastic domain, FEA

NOMENCLATURE

$\boldsymbol{\sigma}$ - stress tensor;
$\boldsymbol{\varepsilon}$ - deformation tensor;
$\boldsymbol{J}$ – Rice integral or deformation energy release rate;
$\boldsymbol{J_x}$,$\boldsymbol{J_y}$ – coefficients from expression of $\boldsymbol{J}$-integral as function of angle of crack extension;
$\overline{T}$ - vector force acting on a infinitesimal surface;
T – T stress
$\boldsymbol{w}$– specific deformation energy;
$\overline{u}$ - displacements vector;
$\boldsymbol{K}$ - stress intensity factor;
$\boldsymbol{G}$– energy release rate;
$\boldsymbol{\delta}$ - CTOD – crack tip open displacement;
α, – crack angle extension;
a – crack length;
c_x – current crack length;
E – modulus of elasticity;
E_{tan} – tangential modulus, for the liniar hardening rule;
σ_y - yielding stress;
R – stress ratio for a variable load;
S_o – opening crack stress;

1. INTRODUCTION

Fracture mechanics defines new criteria and parameters to estimate crack propagation:

$$\boldsymbol{X \geq X_{critic}} \quad (1)$$

where X is a specific parameter, such as: stress intensity factor, K;the energy release rate G, the crack tip open displacement (CTOD), □; or the J-integral, and X_{critic} is the limit value corresponding to crack propagation.

In the crack propagation process, one of the main parameter is the direction of the crack propagation. This assumption was proven by the comparative analysis of the accidents of de Havilland Comet1 [1] jet planes and of the Boeing 737, flight 243 of the Aloha Airlines in 1988[2].

[3] National Research and Development Institute for Gas Turbines COMOTI, Bucharest, Romania

According to the Royal Aircraft Establishment [3], the accident of the de Havilland Comet 1 plane was caused by the propagation, in the transversal direction, of an initial crack of 100 μm. This caused the total damage of the fuselage and all the passengers died in these accidents. In the case of the Boeing 737, a crack was propagated in the longitudinal axis direction of the fuselage and a superior area of the fuselage was broken, but the aircraft landed and only 1 crew member died.

2. THEORETICAL FUNDAMENTS

Crack deflection has been one of the main problems in fracture mechanics. Using Williams' [4] solution for the elasticity problem of a solid with a crack, Erdogan and Shih [5] proposed the maximum circumferential tensile stress criterion. This stated that the crack will grow in a direction normal to the maximum tangential tensile stress. The direction is calculated using a locally maximum condition:

$$\frac{d\sigma_\theta}{d\theta} = 0 \tag{2}$$

which is equivalent with:

$$\frac{K_{II}}{K_I} = \frac{-sin\theta_c}{3 \cdot cos\theta_c - 1} \tag{3}$$

The value of the propagationangle is:

$$\theta_c = 2 \cdot tg^{-1} \cdot \left[\frac{1 - \sqrt{1 + 8 \cdot \left(\frac{K_{II}}{K_I}\right)}}{4 \cdot \frac{K_{II}}{K_I}} \right] \tag{4}$$

Cotterell and Rice [6] demonstrated that the strain energy release rate has a locally maximum for a straight crack extension. For a finite extension of a crack and for small angle deviations, $\Delta\theta$, they proved the following relationship between the stress intensity factors of the initial crack, k_I and k_{II}, and the extended crack, K_I and K_{II}:

$$\begin{cases} K_I = k_I \cdot \left(1 - \frac{3 \cdot \Delta\theta^2}{8}\right) + 0(\Delta\theta^3) \\ K_{II} = -k_I \cdot \frac{\Delta\theta}{2} + 0(\Delta\theta^3) \end{cases} \tag{5}$$

Using the relationship between the stress intensity factors and the energy release rate, they obtained:

$$G = \frac{1}{E} \cdot \left(1 - \frac{\Delta\theta^2}{2}\right) \cdot k_I^2 + 0(\Delta\theta^3) \tag{6}$$

For a mode I regime and using the maximum energy release rate criterion, the crack growth is straight only if:

$$\Delta\theta^2 = 0 \tag{7}$$

The expression of the stress intensity factor in mode II is:

$$K_{II} = k_{II} + 0.5\,\lambda'(x) k_I - \left(\frac{2}{\pi}\right)^{\frac{1}{2}} T \int_0^1 \frac{\lambda'(x)}{(l-x)^{\frac{1}{2}}} dx \tag{8}$$

If the crack is in mode I, the growing path equation, shown in figure 2, is:

$$k_{II} + 0.5\,\lambda'(x) k_I - \left(\frac{2}{\pi}\right)^{\frac{1}{2}} T \int_0^1 \frac{\lambda'(x)}{(l-x)^{\frac{1}{2}}} dx = 0 \tag{9}$$

where T is the T-stress.

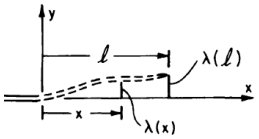

Fig.1Cotterell and Rice model for kinked crack

The maximum energy release rate criterion was proposed by Hussain, Pu and Underwood[7] as function of deflection angle, γ:

$$G(\gamma) = \frac{1}{4E} \cdot \left(\frac{4}{3 + cos^2\gamma}\right)^2 \cdot \left(\frac{1 - \frac{\gamma}{\pi}}{1 + \frac{\gamma}{\pi}}\right)^{\frac{\gamma}{\pi}} \cdot \left\{(1 + 3cos^2\gamma)K_I^2 + 8sin\gamma cos\gamma K_I K_{II} + (9 - 5cos^2\gamma)K_{II}^2\right\} \tag{10}$$

The J-integral was defined by Rice [8] for the following conditions: the crack is positioned on the Ox axis, one ending of the crack coincided with the origin O of the coordinate system and the direction of crack propagation is the Ox axis.

$$J = \oint w dy - \oint \vec{T} \cdot \frac{\partial \bar{u}}{\partial x} dy \tag{11}$$

where, $\bar{u} = u\bar{i} + v\bar{j}$ (the displacements vector);

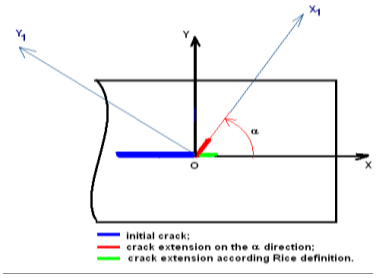

Fig.3 Kinked crack and coordinate system rotation

In the case of a kinked crack, figure 3, Hussam, Pu and Underwood [8] had rotated counter-clockwise the coordinate system by the kinked angle, and had obtained the energy release rate G as function of the crack angle and two contour integral parameters: J_1, the energy release rate per unit crack tip extension on the Ox direction, and J_2, the energy release rate per unit crack tip extension on the Oy direction:

$$G(\alpha) = J_1 cos\alpha + J_2 sin\alpha \tag{12}$$

The kinked angle can be calculated using the maximum energy release rate criterion and the J-integral parameters. The J-integral for a kinked crack becomes:

$$J(\alpha) = J_x cos\alpha + J_y sin\alpha \tag{13}$$

The contour integrals are defined below:

$$J_x = \oint w dy - \oint T \frac{\partial}{\partial x} \bar{u} dy \tag{14}$$

$$J_y = \oint w dy - \oint T \frac{\partial}{\partial y} \bar{u} dy \tag{15}$$

The contour integrals, $J_x$and J_y are constant and depend on theload case and on the structure geometry.
The angle corresponding to the extreme value of the J-integral is calculated from the condition:

$$\frac{dJ(\alpha)}{d\alpha} = 0 \tag{16}$$

$$\frac{dJ(\alpha)}{d\alpha} = (J_x sin\alpha + J_y cos\alpha) \tag{17}$$

Solving equation (20), the value of deflection angle value is:

$$\alpha_0 = arctg\left(-\frac{J_y}{J_x}\right) \tag{18}$$

Tvegaard and Hutchinson [9] had proved, for Mode I, the influence of a negative T-stress on fracture resistance and plastic zone dimension. An approximation of the R curve as a function of T-stress is:

$$J_R = J_{cr}\left(1 - AT\frac{\sigma}{\sigma_y}\right) \tag{19}$$

In expression (19), J_{cr} is the initial value of the material toughness when the crack propagation is initiated, and J_R is the value of the increased fracture toughness at the end of an infinitesimal crack extension (close to the equilibrium state). The T-stress influence on fracture toughness for two stable states is:

$$\begin{cases} J(\alpha, \alpha_i) \cong J_{cr} \\ J\left[\alpha + (\alpha, \alpha_{i+1}) \cong J_{cr}\left(1 - AT\frac{\sigma}{\sigma_y}\frac{\Delta\alpha}{r_p}\right)\right] \end{cases} \tag{20}$$

Equality between the J-integral and the fracture toughness, J_R, means that a change in the geometry caused by a stable growing crack modifies the value of the J-integral corresponding to theequilibrium state of the solid.Subtracting the J-integral values of two consecutive states was obtain:

$$J[\alpha +] - J(\alpha, \alpha_i) \cong J_{Ri} AT \frac{\sigma}{\sigma_y}\frac{\Delta\alpha}{r_p} \tag{21}$$

For an infinitesimally growing crack, expression (21) becomes:

$$\frac{dJ}{d\alpha} \cong -J_{xRi} AT \frac{\sigma}{\sigma_y r_p} \tag{22}$$

Thus, the J-integral in a stable state *(i+1)* is:

$$J_{i+1} \approx J_i exp\left(-\frac{AT\Delta\alpha_i}{\sigma_y r_p}\right) \tag{23}$$

In the first stage, the crack grows for a lower value of the J-integral according to the fracture propagation criteria. As the length of the crack increases, the J-integral will also increase at an exponential rate which is a function of the crack path extension, $\Delta\alpha$.
Fleck and Newman [10] had analyzed the crack closure under plane strain, using a expression of CTOD as a function of T-stress:

$$\boldsymbol{\delta = \frac{K_{max}^2}{\sigma_y E} f(\frac{a\sigma_y^2}{K_{max}^2}, R, \frac{\Delta a\sigma_y^2}{K_{max}^2}, \frac{T_{max}}{\sigma_y}, \frac{\sigma_y}{E}, \nu)} \quad (24)$$

Thus, an indirect influence of the T-stress on the J-integral is shown, when calculated near a stationary crack tip under fatigue loading:

$$\boldsymbol{J \approx \sigma_y \delta = \frac{K_{max}^2}{E} f(\frac{a\sigma_y^2}{K_{max}^2}, R, \frac{\Delta a\sigma_y^2}{K_{max}^2}, \frac{T_{max}}{\sigma_y}, \frac{\sigma_y}{E}, \nu)} \quad (25)$$

Using the model of a crack closure under plane stress for a perfectly plastic material, Fleck and Newman had analyzed the size of the plastic zone for different crack regimes. According to this analysis, there is a 20% difference between the maximum normalized CTOD of a stationary crack and the maximum normalized CTOD of a growing fatigue crack(R=0, $\Delta a = 0.414K_{max}^2/\sigma_y^2$).
If a cyclic load is greater than theopening value, the crack can grow. In terms of the J-integral, the opening ratio is J_0/J_{max} and has a direct influence on the crack growing condition:

$$\boldsymbol{J \geq J_{op}} \quad (26)$$

If the crack is growing, for a opening load deflection angle, the crack growing condition is:

$$\boldsymbol{J_x cos\alpha - J_y sin\alpha \geq J_{op}} \quad (27)$$

Taking into account the condition of maximum energy release rate and the value of the deflection angle, was obtain:

$$\boldsymbol{\sqrt{J_x^2 J_y^2}(cos\alpha_0 cos\alpha + sin\alpha_0 sin\alpha) \geq J_{op}} \quad (28)$$

which is equivalent to:

$$\boldsymbol{cos(\alpha - \alpha_0) \geq \frac{J_{op}}{\sqrt{J_x^2 + J_y^2}}} \quad (29)$$

Using the well-known relationship between the stress intensity factor and the J-integral, the effective stress intensity factor becomes:

$$\boldsymbol{\Delta K_{eff} = \sqrt{2EJ_{max}} - \sqrt{2EJ_{op}}} \quad (30)$$

where J_{max} and J_{op} are the J-integrals calculated for the maximum applied load, S_{max}, respectively for the opening load, S_{op}.

The goals of this paper are to perform a crack path prediction using maximum energy release and the J-integral and to make a comparison with the maximum tangential stress criterion. Also, the influence of the plasticity on the crack path will be analyzed.

3. METHODS TO SIMULATE CRACK EXTENSION

There are many approaches [11] of crack propagation simulation, the difference between them being the methods used for the crack growth prediction (geometry or FEM modeling of the crack growth) and the criteria used to calculate the propagation direction.
In this paper, the crack propagation process is simulated using the J-integral and the maximum of the energy release rate to calculate the angle of propagation. The crack path growth is simulated using FEM modeling – deleting elements along the crack path corresponding to the maximum energy release rate.

For this analysis was used the ANSYS Mechanical 12 solver, 6 nodes PLANE183 triangular elements, without the displacement of the middle nodes towards the crack tip.We use the ANSYS APDL commands to assign the value of the stress and strain displacements tensor components along the curve used to define the J-integral (we define macro-commands to elaborated the geometry and mesh, to calculate J_x, J_y, J and the deflection angle and to perform all the task needed to simulated crack propagation).We had used an edge crack of a plate (figure 4).
An approximation of the stress intensity factor for an edge crack plate is:

$$K_I = \sigma F(\frac{a}{W})\sqrt{\pi a} \quad (31)$$

where,

$$F(x) = 1.99 - 0.41x + +18.7x^2 - 38.48x^3 + 53.85x^4$$

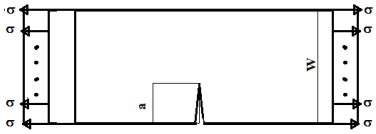

Fig.4 Edge crack plate used to evaluate the precision of the method to calculate J-integral

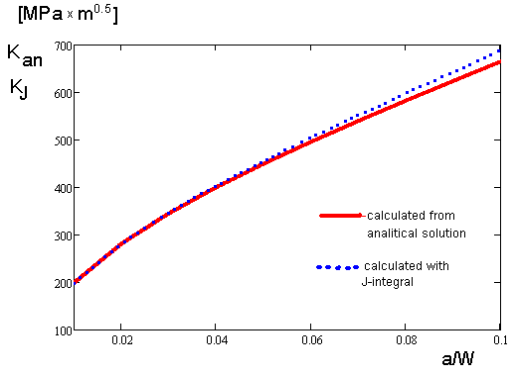

Fig.5 Comparison between stress intensity factor calculated with J-integral and values from analytical solution

The values of the stress intensity factor, calculated with the J-integral, respectively from the analytical solution are shown in figure 5. The errors of the stress intensity factor increase proportionally to the ratio between the crack length and the plate width. For a crack ratio of 1%, the error is of 0.39%, and for a ratio of 1%, the error is of 2.75%.

4. EXPERIMENTAL RESULTS AND DISCUSSION

Using the geometry and the data from real fracture tests, was performed numerical experiments to verify the applicability/validity of this method to predict the crack angle extension (using the maximum energy release rate criterion and the J-integral).

The numerical experiment is performed on the teeth from a helicopter gear box [12]. The real experiment [12] was performed to verify the dependence between the crack propagation direction and the central rim thickness. An initial crack was made at the foot of one of the teeth.

The number of teeth is z=28, the wheel modulus is m=3.2 mm and the width of the wheel is 6.35 mm. The rim thickness is 3.3 times thicker than the tooth height. The wheels are made from consumable electrode, vacuum-melted, AISI 9310 steel. The steel hasthe following mechanical properties: Poisson's Ratio - 0.27; Elastic Modulus – 210 GPA; Yield Strength – 439.5 MPa; Tensile Strength – 820.5.

In the case of two gears in contact, the concentrated force applied on a profile point is generated by tooth contact. The force is applied on the contact point and is normal to the tooth profile, along the contact line which is tangent to the base circles of the gears. The contact point is moving along the tooth profile as the gears are rotating, as per figure 6 causing the variation of the force couple calculated at the crack tip.

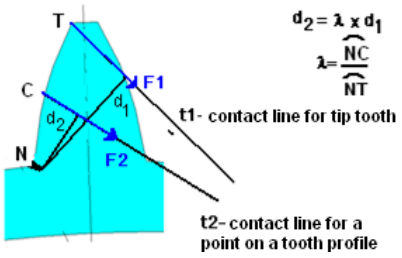

Fig.6 Relative position of the contact line on a rotating gear

Depending on the gear geometry, the couple of the contact force calculated on the gear center is the same:

$$M_m = F_1 r_b = F_2 r_b \quad (32)$$

Thus, the contact force value is the same in every point of the profile: $\boldsymbol{F} = \frac{\boldsymbol{M_m}}{\boldsymbol{r_b}}$

If the force couple is calculated at the crack tip point, a different value is obtained. If the contact point is the tip of the tooth, as in figure 7, the force couple is proportional to the projection of the crack tip on the tangent to the base circle passing through the tooth tip:

$$\boldsymbol{M_{t1}} = \frac{\boldsymbol{M_m}}{\boldsymbol{r_b}} \boldsymbol{d_1} \tag{33}$$

If the contact point is on the profile, the force couple calculated at the crack tip is:

$$\boldsymbol{M_{t2}} = \frac{\boldsymbol{M_m}}{\boldsymbol{r_b}} \boldsymbol{d_2} \tag{34}$$

The projection of the crack tip on a tangent to the base circle is proportional to the length of the profile crack, measured from notch, figure 6. Thus expression (32) became:

$$\boldsymbol{M_{t2}} = \boldsymbol{\lambda M_{t1}} \quad \boldsymbol{\lambda} \in [\mathbf{0}, \mathbf{1}] \tag{35}$$

According to Fleck and Newman, fatigue crack opening occurs for a ratio load of 0.5 ÷ 0.8. Thus, was performed an analysis for two cases: first, for the maximum stress ratio, λ=1, and second, for a 0.5 ratio. If the J-integral was used to calculate the opening stress ratio, to obtain a ratio of 0.5 was necessary to apply a force on a point positioned at 3 quarters of the profile length, measured from the notch, $\lambda = 0.75$.
In Figure 7, is presented the crack path resulted in the test, the crack path predicted with the maximum energy release rate criterion and the J-integral for the elastic and elasto-plastic domains.

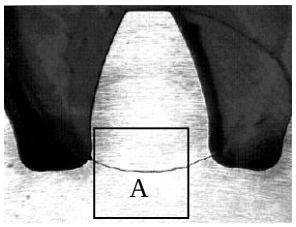

a) Crack path [24]

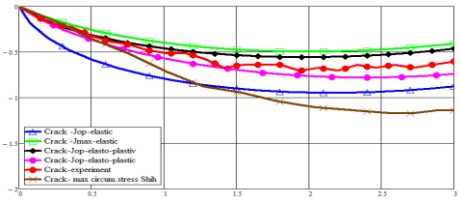

b) Compariton between the crack path of the test specimen and the crack path predictions –detalied view of A zone

Fig.7 Comparison between predictions and test results

In the first stage of crack propagation, x=0÷0.75 mm, the crack path predicted using the maximum circumferential stress and the one predicted using J-integral method (in the elastic field for J=max, and in the elasto-plastic field for both J-max and J-op) are approximately the same. The exception is in the crack predicted with the J-integral in the elastic domain for the opening crack load case. From x=0.75÷1.25 the maximum circumferential stress is more accurate than the J-integral in the elastic domain, only for the opening stress ratio load. For every step of the growing crack, was defined the error function as the distance between the crack path prediction and the crack from the test, divided by the absolute value of the crack tip vertical position.
The error of the maximum circumferential stress criterion increases with the crack length (figure 8). For x greater than 0.75, the crack predicted using the circumferential stress criterion has the lower precision.

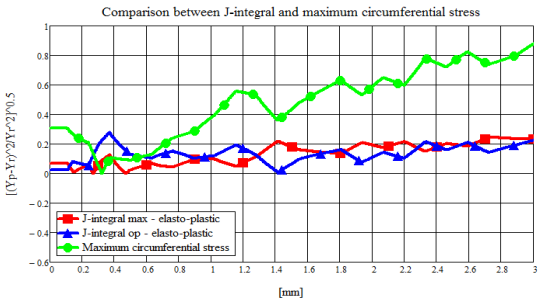

Fig.8 Error function for predicted cracks

The errors of the J-integral method in the elastic-plastic domain increase with the crack length, proving the importance of the Newman equation for the opening stress ratio. If the opening stress ratio is corrected with the crack length, then the precision of the results increases.

5. CONCLUSIONS

Using the J-integral, the predicted crack is in concordance with experimental data. Appling the Newman equation to calculate the initial opening stress ratio and to correct this ratio with the crack length will increase the precision of the J-method.

The area defined by the crack paths predicted with J-integral for loads corresponding to the opening stress ratio, J_{max} and J_{op}, includes the area defined by the crack paths observed on the test specimen. The errors increase after crack length becomes greater than half of the tooth width. According to the error analysis presented in figure 5, the precision of the method used to calculate the J-integral decreases when the ratio between the crack length and the structure width increases.

In comparison to the maximum circumferential criterion, the J-integral is more accurate. The error functions for the J-integral method are two times lower than the error of the maximum circumferential stress, except for the first step prediction, where the error is approximately the same.

ACKNOWLEDGEMENT

The work was carried out within "Nucleu" Program TURBO 2020, supported by the Romanian Minister of Research and Innovation, project number PN 16.26.03.04.

REFERENCES

[1] Withey, P.A. "Failure Analysis Case Studies, vol. II". Elsevier Science Ltd. 2001, pp. 185-191;
[2] National Transportation Safety Board, Aircraft Accident Report, No. AAR-89-03;
[3] Royal Aircraft Estabilshment, "Accident Report 270", Ministry of Supply, London, 1954;
[4] Williams, M. L. "On the Stress Distribution at the Base of a Stationary Crack". Journal of Applied Mechanics, vol. 24, no. 1, 1957, pp. 109-114.
[5] Erdogan, F, Shih, G, C., "Transactions American Society of Mechanical Engineers". Journal of Basic Engineering, December 1963, pp.519-527;
[6] Cotterell, B., Rice, J.,R. "Slightly curved or kinked cracks". International Journal of Fracture, Vol. 16, No. 2, April 1980,pp 155-169;
[7] - Hussain,M.A., Pu.S.L., Underwood,J. "Strain Energy Release Rate for a Crack Under Combined Mode I and Mode II". , American Society For Testing and Materials, 1974, pp 2-28;
[8] Rice, J.R. "A Path Independent Integral and Approximate Analysis of Stress Concentration by Notches and Cracks". Journal of Applied Mechanics, vol. 35, p. 379-376, 1968;
[9] Tvegaard, V, Hutchinson, J.W. "Effect of T-stress on Mode I Crack Growth Resistance in a Ductile Solid". International Journal of Solids Structures, Vol.31, pp. 823-833, 1994;
[10] Fleck, A.,N, Newman, J.,C., Jr. "Analysis of Crack Closure Under Plane Strain Conditions". Mechanics of Fatigue Crack Closure, ASTM STP 982, pp. 319-341, Philadelphia, 1988.
[11] Guidault, P.A, Allix, O., Champaney, L., C. Cornuault "A multiscale Extend Finite Element Method for Crack Propagation". Computational Methods Applied Mechanical Engineering. 197, 2008, pgs 381-389;
[12] David, G., L., Ballarini, R. **"**Effect of Rim Thickness on Gear Crack Propagation Path**"** Seventh International Power Transmission and Gearing Conference sponsored by the American Society of Mechanical Engineers San Diego, California, October 6-9, 19

OVERVIEW OF THE FIRST ROMANIAN SOCIAL SURVEYS ON AIRCRAFT NOISE ANNOYANCE

Adina TOMA[4], Marius DEACONU[4], Luminita DRAGASANU[4], Grigore CICAN[5]

ABSTRACT: It is no longer a "taboo" that people who are exposed to long-term noise may experience annoyance as well as health problems. The European Union has tackled this problem with the introduction of the Directive on Environmental Noise, which obliges Member States to assess and manage noise levels. The Directive is transposed in Romanian legislation and is in force since 2005. But, only drawing up "strategic noise maps" for major roads, railways, airports and agglomerations, using harmonized noise indicators, one cannot assess correctly the number of people annoyed and sleep-disturbed. The paper is presenting the Romanian experience in realizing the first social surveys on aircraft noise annoyance: the implementation of the International Commission on Biological Effects of Noise Procedure, the translation of the two standardized annoyance questions (ISO 15666), the construction of the questionnaire and an overview of a case study performed in vicinity of Iasi Airport. Difficulties, lessons learned and future research will be presented at the end of this paper.

KEYWORDS: social survey, noise annoyance, aircraft noise

NOMENCLATURE

ACARE – Advisory Council for Aeronautics Research in Europe
EU – European Union
END – Environmental Noise Directive
ICBEN – International Commission on Biological Effects of Noise
Leq – Equivalent continuous sound level
NMS – Noise Monitoring Station

1. INTRODUCTION

One objective of the strategic research agenda of the ACARE is to reduce the perceived external noise due to air traffic by 50% until 2020. At the same time the air transport system is, according to ACARE intended to triple the number of its movements by 2020 compared with 2000 and the passenger numbers are expected to double in the next 20 years. One of the ACARE 2050 target state is to reduce the noise annoyance to acceptable levels. The airports must be fully integrated and accepted by local communities. Also, the ACARE is requesting that a full understanding of the level of nuisance, annoyance, sleep disturbance, health effects etc. of emissions, noise and other aviation impacts to be developed [1].

The EU imposed over the years a series of environmental noise policy and related legislation. Since the 1970s, legislative instruments have been developed to regulate noise at the source and in recent years, legislation has transitioned from focusing on the source to mitigating environmental noise at the point of the receiver. This shift has occurred in the context of an emerging evidence base suggesting links between exposure to environmental noise and public health concerns and recognition that concentrating regulation only on the source is not sufficient in itself to alleviate the problem [2].

The "community response to noise" refers to the average evaluation of the noise situation by a "community" or group of residents, combined in a single outcome, annoyance. Annoyance may result from noise-induced disturbance of activities, communication, concentration, rest, or sleep, and may be accompanied by negative feelings such as anger or displeasure (figure 1).

[4] National Research and Development Institute for Gas Turbines – COMOTI, Bucharest
[5] University POLITEHNICA from Bucharest, Faculty of Aerospace Engineering

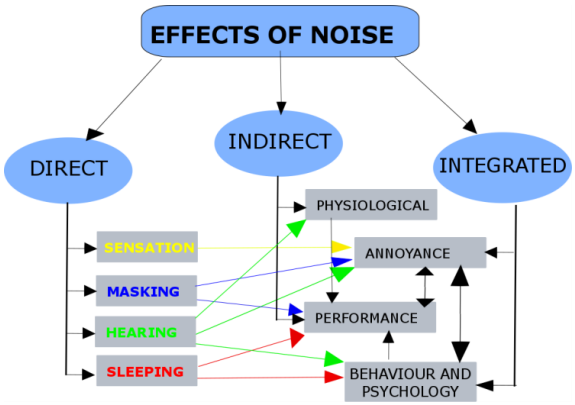

Fig. 1 – Effects of noise on human beings

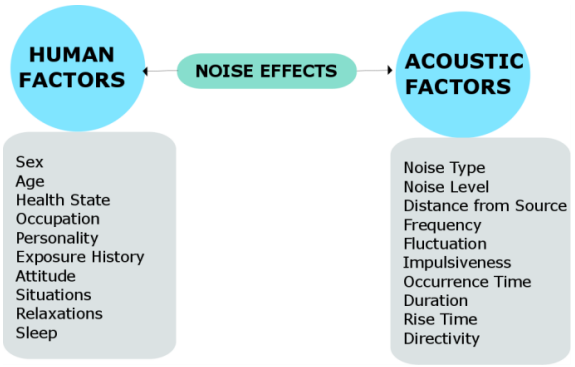

Fig. 2 - Factors influencing effects of noise on human beings

It is an often-forgotten fact that one “does not hear an equivalent level”. In a community noise setting, the noise is perceived as a series of more or less distinct events. It is know that the equivalent level can not describe the noise annoyance situation and different traffic noise situations with the same Leq, may be assessed differently with respect to annoyance, because the factors influencing effects of noise on human beings are both human and acoustic (figure 2).

One of the main objectives of research into the community noise response has been to derive exposure - response relationships. Previously, based on a large international dataset, separate exposure -response curves were derived for aircraft, road traffic, and railway noise [3].

At a given noise level, more annoyance by aircraft noise was found than by road traffic noise (aircraft penalty) and less annoyance by railway noise than by road traffic noise (railway bonus). These relationships are reflected in a EU position paper that has guided EU noise policy [4].

To simplify comparisons of results across surveys and across language barriers, the "community-response-to-noise team" of the International Commission on Biological Effects of noise, ICBEN, developed a set of recommendations for future noise annoyance surveys. They published a set of guidelines for reporting core information from community noise reaction surveys [5], and a few years later two standardized questions were recommended together with standardized response scales [6]. These standardized questions and scales were initially presented in nine languages: English, Dutch (Flemish), French, German, Hungarian, Japanese, Norwegian, Spanish and Turkish. A detailed protocol on how to translate the method into other languages was also presented. The ICBEN recommendation has later been adopted as an international standard, ISO 15666 [7].

In Romania, such kind of research was never done and financed neither by Health Ministry or associated bodies, neither by Environmental Ministry, Environmental Agencies nor by Research Ministry. The only study performed related to this subject is a Study for the development of guidelines to determine dose-effect relations for assessing the annoyance on population, due to the noise from traffic. The budget was around 9000 EUR and was financed by the Ministry of Environment and Forests, in December 2012. A methodology was proposed to develop regulations and guidelines and to establish strategic approach to asses, manage and monitoring the ambient noise including the evaluation of a human response to the estimated discomfort and annoyance. The only financed research connected with “noise subject” was regarding noise reduction at source, phono-absorbent panels and the use of new materials to reduce noise for different applications.

Having all this in mind, knowing the trends in community reaction and the experts point of view on community noise annoyance, COMOTI decided to conduct a small scale research on this field and to perform the first Romanian social survey on noise annoyance.

The paper presents the steps performed and difficulties experienced through this process and off course the objectives for the future work on this field.

2. RESEARCH METHOD

Before starting this research we wanted to see if there is a need to conduct noise annoyance studies connected with air transport in Romania. For this, we get in contact with all Romanian airports and ask them if they received any noise complaints. In parallel, we asked the same thing at the Romanian Civil Aeronautical Authority, the National Environmental Agency and the National Environmental Guard.

From the centralized situation for 2015 we can conclude that from a total of 13 Airports and 2 Major Airfield, only 3 Airports have received complains: Bucharest, Cluj and Iasi and also the Saulesti airfield. What is very interesting, that once with the community complaints connected with flight paths we identified 2 complaints for bees and for birds protected species. Also the Bacau Airport gave us a "politically correct" answer, they said that they fulfill their engagements in compliance with END and according to these results the airport is not disturbing from the noise point of view, but they mentioned that Bacau has also military flights and those are not taken into account according to legislation and in the end of their response they underline the fact that they didn't receive any noise complaints regarding civil aircrafts.

2.1. Implementing the ICBEN Procedure

There is a lack of compatibility between what Authorities sustains and the actual community response to aircraft noise. The first step was to follow the procedure offered by team of ICBEN because the ISO 15666 does not provide the Romanian version of the two standardized noise annoyance questions, even more the standard is not transposed into a Romanian version.

The ICBEN developed a method to construct comparable questions for additional languages that we followed. We chose 21 adverbs and via e-mail we collected 102 answers for minimum and maximum scale, representing words for the highest and lowest level of annoyance.

After this, we prepared the cards and we get 125 responses concerning the intensity score for each remaining adverbs and another set of cards in which they placed their choices for corresponding marks of 25%, 50% and 75%, obtaining the following results: 25% - *putin*; 50% - *nici mult, nici putin* and 75% - *mult*.

What we did additionally for the ICBEN procedure was that after analyzing the data it was observed that some respondents had misunderstood the approach of the proposed questioner, as for example for word "deloc" (English: not at all) it was recorded an intensity score of 82. In order to eliminate this kind of mistakes, an analytical formula, adapted from noise measurements procedure, for the repeatability limit has been implemented, and after applying this procedure for each word the number of valid answers taken into account has diminished. The formulas used are presented bellow:

$$M = \frac{\sum_1^n I_n}{n} \quad (1)$$

$$\sigma = \sqrt{\frac{\sum(I_n - M)^2}{n-1}} \quad (2)$$

$$R = 2.8 * \sigma \quad (3)$$

Where:
I is the intensity score;
M is the mean value;
n is number of valid answers;
σ is Standard Deviation, and
R is the repeatability limit.

For an answer to pass this pre-selection loop the following condition has to be fulfilled: $|I_n - M| \leq R$. In parallel, we've started the translation of the two standardized questions. The original English versions of these questions are as follows:

"Thinking about the last 12 months or so (or alternative time period), when you are here at home, how much does noise from (noise source) bother, disturb or annoy you? Extremely, very, moderately, slightly or not at all?"

"Next is a zero to ten opinion scale for how much (noise source) noise bothers, disturbs or annoys you when you are here at home. If you are not at all annoyed choose zero, if you are extremely annoyed choose ten, if you are somewhere in between choose a number between zero and ten.

Thinking about the last 12 months or so (or alternative time period) what number from zero to ten best shows how much you are bothered, disturbed or annoyed by (noise source) noise?"

Summarizing, we collected 36 English to Romanian translations, 4 France to Romanian translations and 17 back translations and finally we had the 2 standardized questions in Romanian language and the final scale ready to be integrated into the questionnaire. The Romanian questions are:

5 point verbal scale standardized question:

"Luând în considerare ultimele 12 luni, pe perioada cât ați fost acasă, cât de mult v-a deranjat, perturbat sau creat un disconfort zgomotul produs de (sursa). Extrem, mult, nici mult nici putin, putin, absolut deloc ?"

0-10 numerical scale standardized question:

"La următoarea întrebare, notați pe o scală de la 0 la 10 cât de mult v-a deranjat, perturbat sau creat un disconfort zgomotul produs de (sursa) pe perioada cât ați fost acasă. Dacă nu v-a creat deloc un discomfort

alegeţi 0, daca v-a creat un disconfort extrem alegeţi 10, iar dacă sunteţi undeva între aceste două variante alegeţi un număr între 0 şi 10.

Gândindu-vă la ultimele 12 luni, ce număr de la 0 la 10 indică cel mai bine cât de mult v-a deranjat, perturbat sau creat un disconfort zgomotul produs de (sursa)?"

In frame of the 12th ICBEN Congress on Noise as a Public Health Problem, 2017, the Romanian version of the questions were presented [8] and previously, the detailed methodology to obtain the Romanian noise annoyance questions were published in Acta Acustica United With Acustica [9].

2.2. Questionnaire construction

We developed the first questionnaire based on the brief version of the World Health Organization Quality of Life. Because we have been constrained to have a maximum number of items, due to time answering, we organized a focus group to decide what items to be included. Besides the relevant questions of quality of life we included the two standardized questions regarding noise annoyance. In order to differentiate between different sources of noise, we added items that assess not only noise annoyance related to air traffic, but also related to other sources, like car traffic, train, industrial and commercial units.

To validate the questionnaire, we perform an analysis of variance (ANOVA) to test if there are any differences regarding noise annoyance produced by airplanes, ability to concentrate and satisfaction with sleep, between those who live closer to the airport and those who live further. Based on our data, we concluded that there is no significant difference related to afore mentioned variables.

Taking into account the fact that we had just a limited number of participants (8.5%) that declared that they live very close and close to the airport, we performed statistical analysis only for them, using bootstrap method.

The results indicate that those who are disturbed by noise produced by airplanes are also disturbed by noise produced by main road, which sustain the idea that people who are annoyed by noise, in general cannot differentiate between different sources of noise.

Given the fact that a few of the items had no correlation with any other items, we decided to filter them out and not including in the final version of the questionnaire.

So, the first version of questionnaire had 25 questions. In order to validate this questionnaire, we collected data from 408 participants, out of which 90 (22.1%) were males and 318 (77.9%) females, aged between 19 and 75 years old. After the validation process, a second version for questionnaire was obtained having 23 questions.

3. RESULTS AND DISCUSSIONS

3.1. Iasi Airport Case Study

In 2015 there were 3 Romanian Airports with noise complaints. From all of these, Iasi, is in development process, their movements increase continuously, yearly with a 30%, and in 2014 they made a new runway and a new Terminal.

Nevertheless, Iasi is a small airport, easy to work with them, with a real desire to make things correctly from environmental point a view. Also, they have good relations with the local authorities.

After discussing locally we decided that a face-to-face survey is suitable for Iasi.

In order to decide on final area where the social survey will be conducted we consult the noise maps realized for the new runway and the flight tracks (figure 3). The noise map software used is Cadna from Datakustik. From the noise contours we can see that Aroneanu village is more exposed to noise, fact confirmed both by utilization preponderance of the runway 14 to Aroneanu and also by the complaints and movies posted on Facebook. We decided to conduct the social survey also on Valea Lunga village, due to the reason that Iasi Airport had in plan to develop a CARGO line in that direction and we wanted to examine the noise situation to have a reference line.

Regarding the cultural approach we taken into account the possibility to conduct multi-population studies in more languages, is not the case for Iasi, but could be applicable for Transilvania area (Cluj). Within country multiregional research might compare differences among populations in terms of north-south, east-west or urban-rural divisions and this kind of research is needed in the Iasi Airport Case Study.

In period 8-12 September 2015 we received the approvals from the city halls to collect data and conduct the social survey. The social survey was split into two major parts: Collection into the Valea Lunga and into the Aroneanu village. For this action we had also 4 volunteers to help us, so a team of 8 members collected the data.

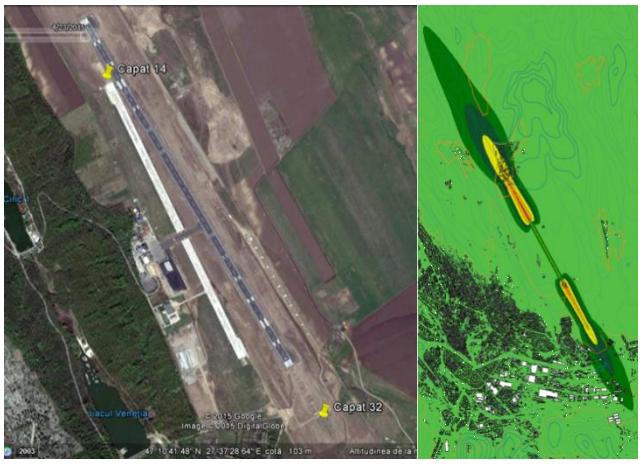

Fig. 3 – Noise contours of the new runway

The survey goal was to obtain one filled questionnaire for each house, regardless if female or male.

At the end of the period we summarized 180 questionnaires from Aroneanu (46,1% male and 53,9% female) and 70 from Valea Lunga (61,4% male and 38,6% female). The statistical analyzes was not performed, but the preliminary results can be observed from figure 4.

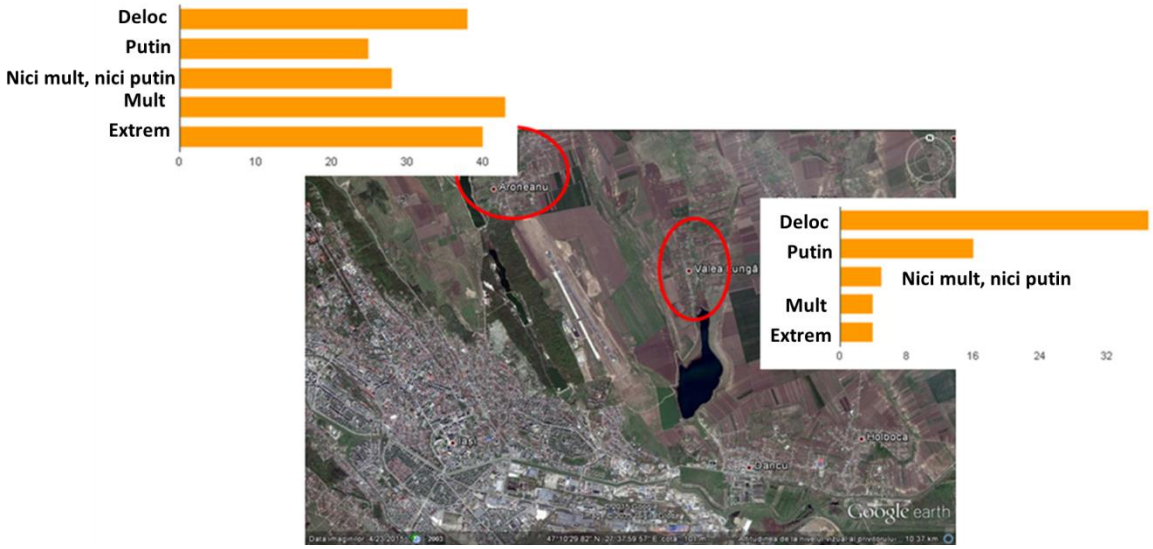

Fig. 4 –Preliminary results obtained from the social survey

The preliminary analyses show us that in Aroneanu are two categories of citizens: one disturbed and annoyed by the aircraft noise and one resigned, especially the older people. Regarding Valea Lunga we can confirm the fact that there is no noise annoyance issue.

4. CONCLUSIONS

When planing a social survey some steps must be followed: preparing the questionnaire with noise annoyance question included, taking into account the cultural approach, taking into account the area in which data will be collected (rural or urban), establishing the relevant area and the correct representative sample from the total population available, the process of collecting the data, transferring all the data collected in an electronic format and finally to perform statistical analysis with high level of confidence.

The main conclusion for the research performed is that we must redesign the questionnaire by reformulating the second standardized question. Also, is needed to simplify the questions, because we used some neologism, but the rural population don't know all the meanings, for example the comfort word was very poor understood by participants. There is a need to reformulate some items. In this version of questionnaire, we put an item with double connotation, pursuing the trend of the response, if the people are positive or negative and if this affect the noise perception, but this item is very difficult to understood by the locals. After the field experience we conclude that we need to reduce the answering options, five options being too much and definitely we need to take into account different questionnaire for different social categories.

Regarding the instructions for interviewers we followed the ISO recommendations, but we need to develop them, especially if there are volunteers involved into collection process. Also a more detailed training for them it is desirable, they need to understand the question and very important to understand the goal of the survey and the importance of the accuracy of responses. For the next steps, definitely we will need to keep more closely the authorities and involve them in more activities.

The next steps for our research on Iasi must focus on analyzing the collected questionnaires with a professional software (ex. IBM SPSS).

Cultural approach in a survey research remains challenging to fund, to organize and monitor, to design, to conduct, and to analyze adequately. The main result after developing a social survey must be the creation of a win-win situation, both for airport and for the community.

ACKNOWLEDGEMENT

This work was carried out within "Nucleu" Program TURBO 2020, supported by the Romanian Minister of Research and Innovation, project number PN 16.26.05.01.

REFERENCES

[1] ACARE Strategic Research & Innovation Agenda - 2017 Update, Volume 1, 2017, http://www.acare4europe.org/sites/acare4europe.org/files/document/ACARE-Strategic-Research-Innovation-Volume-1.pdf ;
[2] E. Murphy, O. Douglas; 2018; Population exposure to road traffic noise: Experimental results from varying exposure estimation approaches; *Transportation Research Part D*; Volume 58; Pages 70-79;
[3] H.M. Miedema, C.G. Oudshoorn; 2001; Annoyance from transportation noise: Relationships with exposure metrics DNL and DENL and their confidence intervals; *Environmental Health Perspect*; 2001; Volume 109; number 4; Pages 409-416;
[4] EU's FUTURE NOISE POLICY, WG2 – Dose/Effect; 2002; Position Paper on Dose-Response Relationships between Transportation Noise and Annoyance; ISBN 92-894-3894-0;
[5] J.M Fields, R.G.de Jong, A.L.Brown, I.H. Flindell, T.Gjestland, R.F.S. Job, S. Kurra, P. Lercher, A. Schumer-Kohrs, M. Vallet,T. Yano; 1997; Guidelines for reporting core information from community noise reaction surveys; *Journal of Sound and Vibration*; Volume 206; Pages 685-695;
[6] J.M. Fields, R.G. de Jong, T. Gjestland, I.H. Flindell, R.F.S. Job, S. Kurra, P. Lercher, M. Vallet, T. Yano, R. Guski, U. Felscher-Suhr, R. Schumer; 2001; Standardized General-Purpose Noise Reaction Questions for Community Noise Surveys: Research and a Recommendation; *Journal of Sound and Vibration;* Volume 242; Pages 641– 679;
[7] International Organization for Standardization; 2003; Acoustics – Assessment of noise annoyance by means of social and socio-acoustic surveys; ISO/TS 15666:2003 (reviewed and confirmed 2013);
[8] T.Gjestland; 2017; Standardized general-purpose noise reaction questions; ICBEN; 12th ICBEN Congress on Noise as a Public Health Problem; Zurich; 18-22 June 2017; Page 1-8
[9] T.Gjestland, A. Toma, L. Dragasanu, M. Deaconu, B. Oprea; 2017; Romanian Standardized Noise Reaction Questions for Community Noise Surveys; Acta Acustica United With Acustica; Volume 103; Pages 1-4.

WIRELESS VIBRATION HARVESTING SYSTEM FOR TURBINE ENGINES

Cristian Valentin NECHIFOR[6], Adrian STOICESCU[6], Romeo Dorin HRIŢCU[6]

ABSTRACT: The article presents the operation and testing of a vibration energy harvesting system with a piezoelectric harvester and wireless sensor data transmission. Conceiving a system that not only includes vibration harvesting on a turbine engine but also a wireless instrumentation node, is a matter of insufficient development maturity within worldwide research area. Within this paper, we proposed and tested, in the lab and on a turbine engine, an architecture for an autonomous instrumentation system, with wireless communication and powered by energy from vibration.

KEYWORDS: harvesting system, piezoelectric, vibrations, turbine engine, wireless instrumentation

NOMENCLATURE

P – maximum power achieved [W], P_ω – mean power available for the harvester [W], Y – case displacement (maximum vibration amplitude) [m/s^2], f – frequency [Hz], k – spring constant, m – mass [g], ζT – total damping factor, ω – vibration frequency [Hz], ω_r – device resonant frequency [Hz]

1. INTRODUCTION

Turbomachinery automation begins with control systems for fuel delivered to the combustion chamber and goes up to total control of their operation, implying a vast complex of elements that do a wide range of processes needed for overall operation of the whole machine system. Auxiliary systems involved concentrate technologies that have an increasing demand for efficiency and improvement.

Autonomous instrumentation becomes a research and development area of large interest worldwide. The articles cited within this work, innovations of some manufacturers, as well as directions imposed by European-financed R&D projects, are proof of this. Our project had in mind from the beginning to meet these concernments and bring its own contribution, with an emphasis on turbomachinery applications.

Both in aerospace and industrial or ground-tested turbomachinery, innovations are studied with the aim of saving and reusing produced energy. The paper presents fundamental aspects of piezoelectric devices and towards the end the results of tests with our system.

2. VIBRATION ENERGY HARVESTING SYSTEMS

The vibration harvesting process represents one of the research directions towards increased energy efficiency of electric systems, increased autonomy of measurement nodes in hardly accessible locations and decreased overall system mass by eliminating cables and power adapters. In the context of improving control systems for turbomachinery, an example of a turbine engine was analyzed with the aim of integrating a piezo harvesting system solution. First, research was necessary for examining the possibility of converting vibration energy into electrical energy. The most important aspects are: the structure and properties of piezoelectric generators, harvesting networks, integration and optimization.

Even if the vibration energy of a machine, in proper operation in relation to its application, is reduced, it could be used for powering up low-power electronics, thus leading to a separation of electrical circuits and a decrease

[6] National Research and Development Institute for Gas Turbines COMOTI, Bucharest, Romania

of auxiliary consumption impact upon power allocation. Therefore, steps are made towards complying with international requirements regarding energy consumption efficiency.

The advantages of recovering losses and using unconventional energies are recognized worldwide. Vibration harvesting not only contributes to minimizing system losses, but also increased the technology level, opening the path for high-end technologies such as compact or autonomous control systems.

Vibration energy harvesting systems can be one of the main forms of a self-powered dynamic system. This is defined as a dynamic system powered but its own excess of kinetic and/or renewable energy [1]. The concept of self-powered system is shown in Fig. 1. In the case of machinery, excess movement (vibration) is harnessed, its energy being able to generate electric current to power various subsystems.

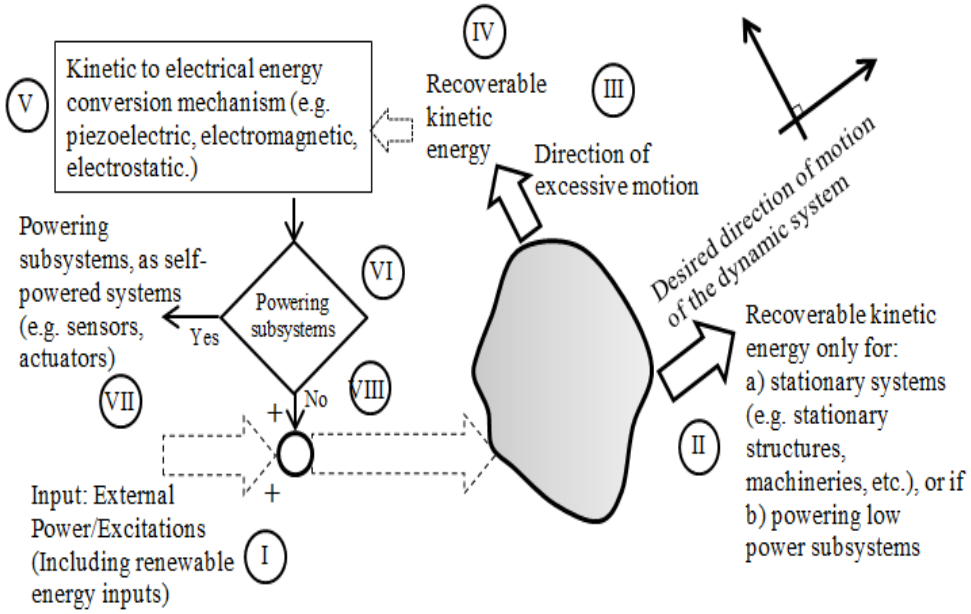

Fig. 1 The concept of self-powered dynamic systems [2]

Faults or malfunctions in a rotating machine produce mechanical oscillations with frequencies higher (often integer multiples) than the machine speed [3]. They can occur from multiple reasons such as: cog friction, bearing irregularities, turbine and compressor blade movement, rotor eccentricities or misalignments. By studying the Fourier spectrum of measured vibration, one can determine the vibration causes, but as long as there are moving elements, vibration can never be fully eliminated. Networks that harvest its energy, adjusted for that spectre, can make use of this excess which is otherwise wasted and not recovered.

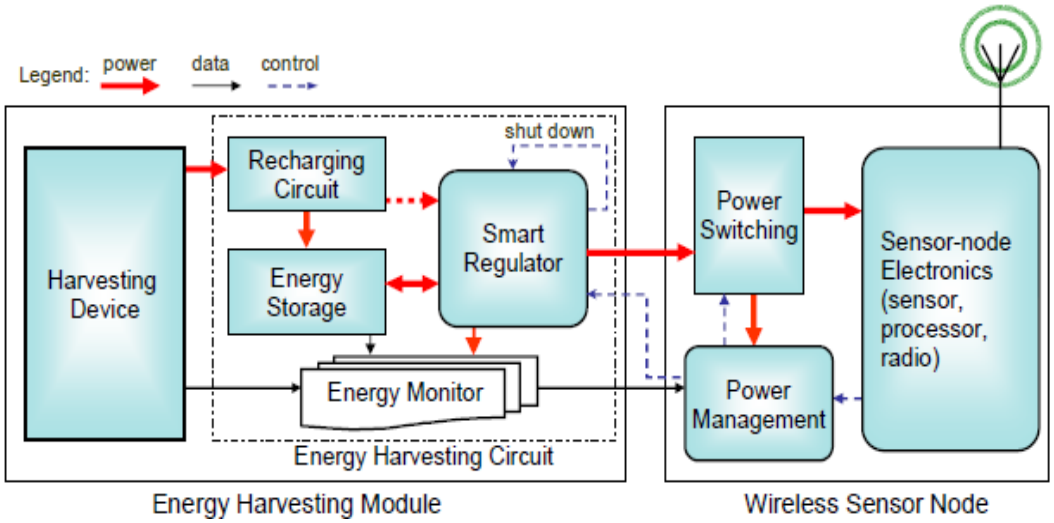

Fig. 2 Energy harvesting system for powering a wireless sensor node [4]

Self-powered sensors require an architecture of energy harvesting modules, that includes both the harvester device and its circuit. Besides that, a power management subassembly is needed. Fig. 2 illustrates a diagram by which the energy harvesting module produces, controls and delivers power from the existing vibration to a wireless sensor node.

The advantage is the lack of cables both for powering the node and data transmission, namely a lack of physical connection of the assembly with the exterior. There is also another advantage: integration into hardly accessible or isolated locations, such as aerospace systems.

3. STRUCTURE AND PROPERTIES

For machinery vibration energy harvesting, mostly linear devices based on inertial mass systems were used [5]. The general model is the one in Fig. 3, consisting of an inertial mass (m), a spring (k) which connects the mass (m) to the casing and damper that represents the energy conversion mechanism. When a harvester vibrates with the vibration source, the inertial mass moves out of the phase of its casing, resulting in a displacement or bending between the casing and the mass.

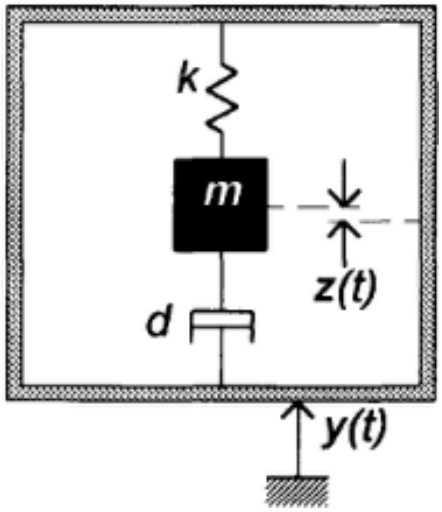

Fig. 3 Diagram of a simple generator of electricity from vibration energy [6]

The mean power available for the harvester, which includes both power to the electric loads and power dissipated by mechanical damping, is as follows: [5][6]:

$$\boldsymbol{P}_{(\omega)} = \frac{m\zeta_T Y^2 \left(\frac{\omega}{\omega_r}\right)^3 \omega^3}{\left[1-\left(\frac{\omega}{\omega_r}\right)^2\right]^2 + \left[2\zeta_T - \frac{\omega}{\omega_r}\right]^2} \tag{1}$$

where ζ_T is the total damping factor, Y the casing displacement (maximum vibration amplitude), ω is the angular vibration frequency, and ω_r is the resonant frequency of the harvester. Linear harvesters have a specific resonant frequency, which is designed to achieve a high quality factor. When the resonant frequency matches the vibration of the source, maximum power can be achieved [5]:

$$\boldsymbol{P} = \frac{mY^2\omega_3^3}{42\zeta_T} \tag{2}$$

It can be seen that the power decreases as the resonant frequency falls out of the match with the vibration source. This limits the development of linear harvesters. Typically, there are two workaround methods for this problem [7]. One is frequency tuning of the harvester so that the resonant frequency matches the ambient vibration. To that effect, one needs to change the structure's mechanical properties or electrical loads. Tuning can act either continuously or recurrently.

Harvester frequency tuning can be performed using a tuning actuator [8]. Actuators can be continuously active or not (sometimes called passive) [7], in which case they keep the resonant frequency during the inactive time also. Active actuators can be, for example, some electrostatic springs [9], while passive actuators can be various flexing mechanisms.

4. PIEZOELECTRIC SYSTEM PERFORMANCE ON A TURBINE ENGINE

Testing on a turbine engine consists of attaching the harvester on the engine case, connecting it to a harvesting board and measuring voltage generated during the engine operation.

The engine ran between 10,500 and 12,000 rpm, at various regimes and speed levels, while information regarding generated voltage, engine speed (frequency) and vibration were continuously monitored. The rectified output voltage of the harvester was measured in respect with associated vibration values.

Vibration and voltage measurement was performed using the 01dB Orchestra multichannel data acquisition system. They were made in order to test and determine the response of the harvester in real conditions, as well as the influence of the vibration on generated voltage. For the signals from the accelerometers, a FFT function was applied, from which only the spectral component of the compressor was extracted.

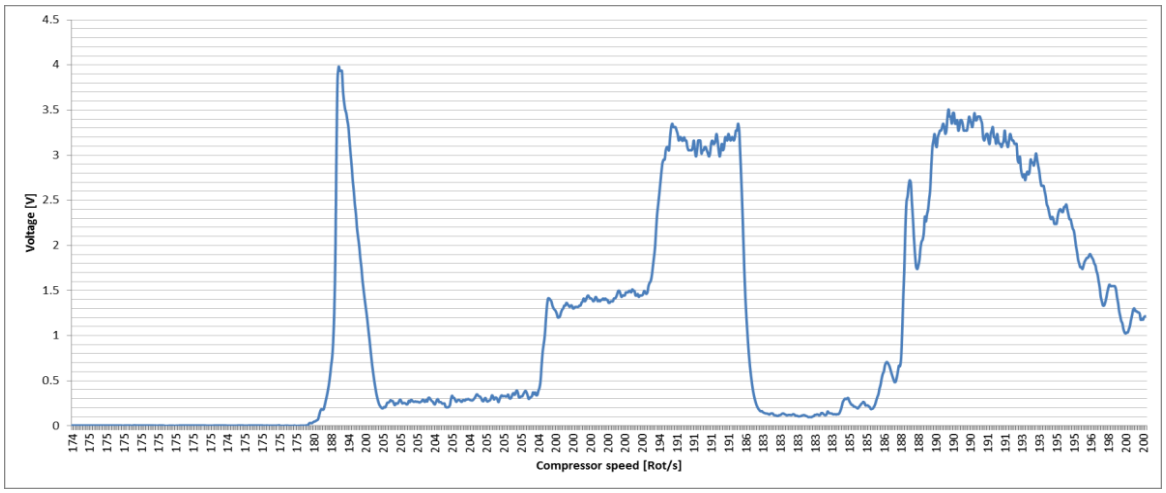

Fig. 4 Voltage (V) associated with the engine speed (rot/s; Hz)

A vibration of nearly 0.9 g was measured at the frequency of 190 Hz (11.400 rpm). At the resonant frequency, the recorded voltage was between 3 and 3.5 V, as seen in Fig. 4, above the level of a small-sized battery.

In Fig. 4, where voltage is illustrated with the engine speed, it can be seen that, during transient regime, a value of 4 V was obtained at 190 Hz.

It is important to know the reason why we obtained some differences during lab testing with the vibration shaker. These showed the harvester resonance at 205 Hz, higher that on the engine. This may be due to the assembly attachment. When testing on the shaker, the harvester was attached with screws, while on the engine it was done with magnets. Magnets do not have the stiffness of the screw attachment. This led to a decrease in the resonant frequency, according to the following equations:

$$f = \sqrt{\frac{k}{m}} \tag{3}$$

where f – frequency, k – stiffness constant and m – mass.

Following the experiments, it was observed that the harvester is quite sensitive to screw fixation. The stiffness can thus vary quite a bit. A fixation variation with only 90° was enough to change the frequency by 15-20 Hz.

In order to use the energy harvested from the environment, it is fundamental that the energy consumed is lower or equal than the energy produced. With this principle in mind, one can try to obtain as much energy

as possible from turbine engine vibration, both by reducing load consumption and developing a smart power delivery management.

With the aim of developing a system that can perform wireless transmission of data from sensors, we used the evaluation kit P2110-EVAL-01 from 'Microchip', as seen in Fig. 5. This includes a data acquisition module, developed with the PIC24F16KA102 microcontroller, which can acquire data from local sensors (temperature, light, humidity) and wirelessly send it using a second module, developed with MRF24J40, specialized on 2.4 GHz communication according to the standard IEEE Std 802.15.4™-2011 "Low-Rate Wireless Personal Area Networks" (LR-WPANs).

¶ (12 pt)

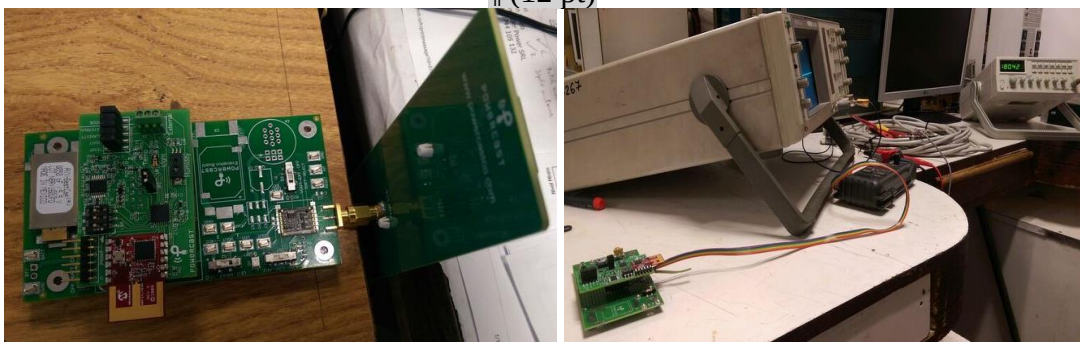

Fig. 5 Lab testing

The energy released by the host system, which is lost from the useful process, during normal operation, can be harnessed by the harvester and transformed into electrical energy for powering data acquisition and transmission circuits.

Improving this circuit was made by introducing a chosen capacitor, with very low losses, to consume as low of the harvested energy as possible. This insures stored power needed in selected moments of data acquisition and transmission. The ratio between the capacitor load time and consumption time (when the useful circuit is active; sleep time and run time of the acquisition and transmission microcontrollers) was conveniently chosen, so that the circuits would run for 10-12ms every 20-30s (ratio 1/2000).

For maximum reduction of the consumption we did as follows:

In the data transmission mode we selected for the active time the TX (data transmission) mode with a consumption of 23 mA but for only 10ms.

During the pause time, for storing harvested energy, that lasts for 33s, we set the transmitter in the Sleep mode, with a consumption of only 2 μA, which influences vibration energy storage process the least.

1. CONCLUSION

Regardless the method and the amount of maximization of harvested energy, it is fundamental to find ways for a smart management of useful consumption. This way, the consumption of data acquisition and transmission needs to be optimized by programming operation modes and temporizing them according to the speed and rhythm of the energy harvesting process.

Having an energy source that can deliver static energy, enough for use, an energy storage device at level x% from 100% in a specific time, we can use the stored energy in a shorter time for our consumption, reducing the storage to the minimum needed for proper operation (y%, e.g. 30%). After consuming the energy down to this limit, then comes a reload time up to level x% of the power capacity for the loads, during which useful consumption is drastically limited or cancelled.

Future studies in this area can be made to find modeling methods for the load, with the aim of economically and efficiently using harvested energy - control, temporizations, optimizations.

ACKNOWLEDGEMENT

This work was carried out within "Nucleu" Program TURBO 2020, supported by the Romanian Minister of Research and Innovation, project number PN 16.26.07.01.

REFERENCES

[1] V.V. Vantsevich, M.V. Blundell; 2015; Mechatronics of Vehicle Control and Self-powered Systems; *Advanced Autonomous Vehicle Design for Severe Environments*; Volume 44; Publisher IOS Press; Amsterdam; p. 320.
[2] F. Khoshnoud, Y.K. Chen, R.K. Calay, C.W. de Silva, H. Owhadi; 2013; Self-Powered Dynamic Systems; European Conference for Aeronautics and Space Sciences (EUCASS); Munich, Germany; 1-5 July 2013; p. 3.
[3] Clarence W. de Silva; 2006; *Vibration: Fundamentals and Practice*; 2nd edition; CRC Press Taylor & Francis Group; Boca Raton, USA; pp. 579, 638.
[4] Lei Wang; 2007; *Vibration Energy Harvesting by Magnetostrictive Material for Powering Wireless Sensors*; North Carolina State University; Chapel Hill, USA; p. 4
[5] Dibin Zhu; 2011; Vibration Energy Harvesting: Machinery Vibration, Human Movement and Flow Induced Vibration; Edited by Yen Kheng Tan; *Sustainable Energy Harvesting Technologies – Past, Present and Future*; Publisher InTech; London – UK; pp. 26, 27
[6] C.B. Williams, R.B. Yates; 1995; Analysis of a micro-electric generator for microsystems; Sensors and Actuators A; Proceedings of the 8th International Conference on Solid-State Sensors and Actuators Eurosensors IX (IEEE Xplore); Stockholm, Sweden; 25-29 June 1995; p. 369.
[7] D. Zhu, M.J. Tudor, S.P. Beeby; 2010; Strategies for increasing the operating frequency range of vibration energy harvesters: a review; *Measurement Science and Technology*; Volume 21; Nr. 2; Publisher, IOP Publishing Ltd; Bristol, UK; pp. 2,3.
[8] S. Roundy, Y. Zhang; 2005; Toward self-tuning adaptive vibration based micro-generators; Smart Structures, Devices and Systems II, Proceedings; SPIE; Volume 5649; Bellingham, USA; 28 February 2005; pp. 273, 278.
[9] S.G. Adams, F.M. Bertsch, K.A. Shaw, P.G. Hartwell, F.C. Moon, N.C. MacDonald; 1995; Capacitance based tunable resonators; Proceedings of the 8th International Conference on Solid-State Sensors and Actuators Eurosensors IX (IEEE Xplore), Stockholm, Sweden; 25-29 June 1995; pp. 438, 439.

Additive manufacturing technologies available in COMOTI.

LASERTEC 30SLM

Selective laser melting machine with metallic powder.

ProJet 1200

Stereolithography (SLA) system using UV curable polymers.

Dimension Elite

Material extrusion system using ABS.

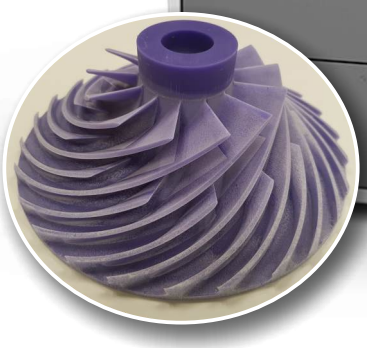

ProJet 3600W

Material jetting system using wax.

COMOTI

The only specialized company that integrates such activities as

scientific research,
design,
manufacturing,
testing,
experimental activities,
technologic transfer and
innovation

in the field of aircraft and industrial gas turbines and high speed bladed machinery.

220D Iuliu Maniu Ave., 061206 Bucharest, ROMANIA,
P.O. 76, P.O.B. 174
Phone: (+4)021/434.01.98, (+4)021/434.02.31, (+4)021/434.02.40
Fax: (+4)021/434.02.41, e-mail: contact@comoti.ro

www.comoti.ro